Title page with author details

Integrating spatio-temporal analysis for assessing the effectiveness of POLARIS in Arctic shipping traffic

Yaqing Shu[a,b], Wenyang Xu[b], Hailong Cui[b], Jinli Xiao[a,b], Lan Song[c*], Huanhuan Li[d], Zaili Yang[d]

[a] State Key Laboratory of Maritime Technology and Safety, Wuhan University of Technology, Wuhan, China

[b] School of Navigation, Wuhan University of Technology, Wuhan, China

[c] College of Engineering, Eastern Institute of Technology, Ningbo, China

[d] Liverpool John Moores University, Liverpool, UK

*Corresponding author: lansong@eitech.edu.cn

Integrating spatio-temporal analysis for assessing the effectiveness of POLARIS in Arctic shipping traffic

Abstract

The annual reduction in Arctic sea ice extent has driven a steady increase in shipping activities, which has put forward higher requirements for the navigation safety and management of ships in the Arctic. To address these challenges, the International Maritime Organization published the Polar Operational Limit Assessment Risk Indexing System (POLARIS), which introduces a sea ice risk quantification model and proposes operational restrictions for ships in different ice conditions. In this study, Automatic Identification System and sea ice data from 2018 to 2022 in Arctic were spatio-temporally correlated to assess the effectiveness of the POLARIS in guiding ship navigation. The findings reveal that the ship trajectories and speed are significantly influenced by sea ice conditions, and non-compliance with the POLARIS is evident among ice-class ships. In high-risk operating waters, the non-compliance rate of PC4, PC6, and PC7 ice-class ships is nearly 70%, and the median exceedance magnitude is approximately 3.25 kn. By analyzing non-compliance events and ships entering areas requiring special operations, high-incidence areas of non-compliance for ice-classes ships were found, with the highest-incidence areas occurring in the Kara Strait and in the areas of northwest of Svalbard. Temporally, most non-compliance events were concentrated between January and June, and again in December. These results indicate that the POLARIS may require revision to better reflect and support real-world

navigational behavior in Arctic waters and ship-specific risk factors. This study provides a critical theoretical policy-making solution to improving the POLARIS, thereby enhancing ship safety and the effectiveness of regulations in ice-covered waters.

Keywords: Arctic shipping; POLARIS; effectiveness assessment; navigation risk; shipping traffic

1. Introduction

Against the background of global warming, the Arctic is warming faster than the global average, a phenomenon known as Arctic amplification (He et al., 2024). This will accelerate the melting of Arctic sea ice and make the ice layer thinner. According to the National Snow and Ice Data Center (NSIDC), the Arctic sea ice extent has shown a sustained decline since 1979, with the reduction being particularly pronounced during summer (Zhang et al., 2025). International organizations involved in climate observation and maritime management have determined that the reduction in sea ice extent has led to an extended Arctic summer ship navigation period and increased navigable waters (Cao et al., 2022; Diebold et al., 2023; Lindstad et al., 2016). In addition, a comprehensive assessment and comparison of the safety, economics and geostrategic implication of the Arctic Route and the Suez Canal Route by relevant scholars shows that the Arctic Route can serve as a viable alternative and has many advantages (Shu et al., 2023; Akbayirli and Okan, 2022). Consequently, an increasing number of ships are entering the Arctic for maritime operations (Koçak and Yercan, 2021; Lin et al., 2024). However, differences in ship structural strength and icebreaking capabilities result in varying levels of sea ice tolerance (Tarovik et al., 2022). Moreover, the spatio-temporal distribution and dynamic movement of sea ice in different Arctic areas will affect the ship's maneuvering behavior and route selection (Lin et al., 2024).

The 2024 North Sea Route (NSR) ship navigation report published by the Centre for High North Logistics (CHNL) indicated that the number of ships transiting the NSR

has been continuously increasing from 2015 to 2024 (CHNL, 2024). The voyage number of ship transits was recorded to have risen from 18 in 2015 to 97 in 2024, while the cargo volume was reported to have grown to 3.1 million tons, representing a historical maximum. In light of the increasing number of transiting ships, higher demands have been placed on Arctic ship management regulations to ensure the safety and efficiency of navigation. Management rules and legal guidelines for Arctic ship navigation have been promulgated by relevant countries and organizations. For instance, the Sea Ice Nomenclature (SIN) and the Egg Code have been published by the World Meteorological Organization (WMO), the Arctic Ice Regime Shipping System (AIRSS) by Canada, and the Polar Operational Limit Assessment Risk Indexing System (POLARIS) by the International Maritime Organization (IMO), all of which are regarded as regulatory references for the safety and management of Arctic navigation (Bond et al., 2018; Chen et al., 2025). Among these, the POLARIS is considered the most widely applied risk decision-making tool for Arctic ship navigation (Li et al., 2022). It has a detailed classification of ship icebreaking levels and provision of speed limits under varying sea ice risk. However, the operational recommendations provided by POLARIS, particularly its speed limits, have not yet been quantitatively evaluated against real-world navigation. Therefore, assessing ship compliance with the POLARIS during navigation based on historical Arctic sea ice and ship navigation data is an important way to verify the applicability and effectiveness of the rules. Here, POLARIS effectiveness is defined as the extent to which its guidance is adopted in practice.

Operations within the recommended speed limits are classified as compliant, whereas speeds exceeding these limits are classified as non-compliance events, indicating non-adherence to guidance rather than a breach of mandatory regulations.

The remainder of this paper is structured as follows. In Section 2, a systematic literature review is presented, and the research gaps and study contributions are identified. In Section 3, the data sources and preprocessing procedures are described, and methods for data fusion and for assessing the effectiveness of POLARIS are presented. In Section 4, the spatio-temporal analysis of Arctic shipping traffic is presented, and the POLARIS compliance across different ice-class ships is assessed. In Section 5, a comprehensive discussion and corresponding policy responses are provided. Finally, the conclusions of the study are presented in Section 6.

2. Literature review

In this section, relevant policies affecting ship navigation safety in Arctic ice-covered waters and their evolution are first reviewed. Then the shortcomings of current research and the contributions made by this paper are listed by summarizing the relevant literature.

2.1 Guiding policies related to Arctic shipping

Before the POLARIS was promulgated, the governments of Canada and Russia established their own ship risk assessment systems for the special ice conditions in their Arctic waters. Relevant scholars have conducted some assessments regarding the application and guidance effectiveness of these systems.

Canada initially introduced the Zone/Date System (Z/DS) in 1985 based on the natural law of Arctic sea ice and the practical experience of ship operators (Canada, 2010). This system divided Canadian Arctic waters into sixteen Shipping Safety Control Zones and specified navigable windows for each of nine Arctic Class ships and five type ships within these zones. However, the fixed mode of the system could not cope with the increasingly changing sea ice environment conditions (Bond et al., 2022). Therefore, Transport Canada introduced a more flexible AIRSS as a supplement and expansion of Z/DS in 1996 (Kubat et al., 2005). AIRSS assesses whether a ship can enter the target ice area based on the value of the Ice Numeral (IN). If $IN \geq 0$, the ship is permitted to proceed normally, whereas if $IN < 0$, the risk is deemed too high for further progression. The calculation rule of IN is as follows: $IN = (C_1 \times IM_1) + (C_2 \times IM_2) + (C_3 \times IM_3) + \cdots + (C_n \times IM_n)$, where $C_1, \cdots, C_n$ are the Sea Ice Concentration (SIC) of different waters, and IM are the corresponding Ice Multipliers for each ice-class ship type, which is divided as shown in Table 1. Until 2016, AIRSS was recognized as the leading methodology for assessing ship navigability in Arctic waters in northern Canada (Copland et al., 2021). As a result, many researchers have used AIRSS to assess the impact of sea ice changes on ship navigation safety and route selection in the Northwest Passage (NWP) (Aksenov et al., 2017; Howell and Yackel, 2004; Timco and Kubat, 2001). Since the International Code for Ships Operating in Polar Waters, abbreviated as the Polar Code, became effective in 2017, a new law, the Arctic Shipping Safety and Pollution Prevention Regulations

(ASSPPR), has been passed and implemented in Canada. The new rules retain the use of Z/DS for regional management and AIRSS for quantifying sea ice risk, while adding ice-class ship type classification to adapt to the POLARIS (Solski, 2023).

Table 1. Ice Multipliers (IM) (Transport Canada, 2018)

Ship Category	Open Water	Grey Ice	Grey White Ice	Thin First Year 1st Stage	Thin First Year 2st Stage	Medium First Year	Thick First Year	Second Year	Multi Year
CAC 3	2	2	2	2	2	2	2	1	-1
CAC 4	2	2	2	2	2	2	1	-2	-3
Type A	2	2	2	2	2	1	-1	-3	-4
Type B	2	2	1	1	1	-1	-2	-4	-4
Type C	2	2	1	1	-1	-2	-3	-4	-4
Type D	2	2	1	-1	-1	-2	-3	-4	-4
Type E	2	1	-1	-1	-1	-2	-3	-4	-4

In 2013, the Ministry of Transport of the Russian Federation issued a specialized regulation for the NSR to manage ship navigation and operating behavior, titled Rules of Navigation in the Water Area of the Northern Sea Route (hereinafter 2013 Rules) (Bartenstein et al., 2022). Compared to the Rules of Navigation on the Seaways of the Northern Sea Route issued by the Ministry of Maritime Fleet of the USSR in 1990, the most significant change is the abolition of the compulsory pilotage system, which allows foreign ships to navigate independently along the NSR (Vylegzhanin et al., 2020). The 2013 rules are based on the Russian Ice Certificate, which divides the navigable windows and corresponding navigational restrictions for ships of different ice-classes, while distinguishing whether to provide icebreaker assistance (Bhagwat and Khalturinskaya, 2023). Based on the classification of ice-class ships in the Russian Ice Certificate, the 2013 rules further divided ice-class ships into four categories

(Todorov, 2022). Category 1, ships without an ice-class and those with ice-classes ranging from Ice1 to Ice3. Category 2, ships with ice-classes Arc4 to Arc9. Category 3, icebreakers with ice-classes Icebreaker6 to Icebreaker7, and Category 4, icebreakers with ice-classes Icebreaker8 and Icebreaker9. Subsequently, the latest version of the navigation rules was updated in 2020 (hereinafter 2020 Rules) (RFGD, 2020). Similar to the Z/DS division of zone management, the 2020 Rules has also divided its NSR into boundaries and 28 areas, and has established an optimal navigation window from July 1 to November 15 based on ice-class of the ship. The 2020 rules clarified whether the route is passable with or without the assistance of icebreakers, and under four types of ice conditions: heavy, medium, light ice conditions, and clean water. Many scholars have previously studied the application of the regulations to ship activities along the NSR. It has not only been used to explore the correlation between ship navigation behavior and sea ice conditions in NSR waters (Yakimov, 2023), but also to conduct in-depth research on the navigation safety and efficiency of ships on ice based on the Ice Certificate (Kulesh et al., 2013). In addition, it has also been used to assess the overall safety status of ship navigation on the NSR (Marchenko, 2014).

Due to the complexity of the regulatory framework for Arctic waters, the adoption of the POLARIS is considered to have redefined the standard for Arctic waters regulation (Mudryk et al., 2021). The POLARIS integrates the risk assessment systems established by Canada and Russia in the NWP and the NSR. In the meantime, the POLARIS follows the concept of ice regime proposed by Canada's AIRSS, and

quantifies the risks that different ice-class ships may face under various sea ice conditions through the Risk Index Outcome (RIO). The calculation of the RIO value is similar to the IN value, but with a more sophisticated management approach to the risk of ships encountering sea ice. The POLARIS is unique in explicitly recognizing speed as a key factor affecting safety in ice-covered waters, thus dividing sea ice risk intervals for high-risk and special operations with appropriate recommended actions for navigation (Bond et al., 2018). Therefore, the POLARIS is widely used as a universal risk assessment tool for Arctic ship navigation.

Over the past decade, the number of ships transiting the Arctic has increased by 37% (Boylan, 2021). This rise in traffic has spurred research on navigation risk assessment using the POLARIS as a key analytical tool (Fedi et al., 2018b). Several studies have combined AIS data with sea ice observations to evaluate how different ice-class ships navigate ice-covered waters (Fedi et al., 2018a). Browne et al. (2022) verified the guidance effect of POLARIS on a Polar Class 5 (PC5) ice-class ship sailing in NWP based on the expert evaluation method. In addition, the researchers have introduced the POLARIS assessment of sea ice risk to Arctic ship navigation (Lee et al., 2021; Liu et al., 2020). Jiacai et al. (2025) assessed navigation risk using POLARIS for ships transiting the Northwest Passage (NWP), and Arctic ship accessibility was examined by Chen et al. in terms of the influence of constraints informed by POLARIS (Chen et al., 2023). Building on the risk calculation framework and recommended speed limits provided by POLARIS, a growing body of work has incorporated these outputs

as operational constraints in Arctic route planning. For example, Wang et al. (2025) proposed an incremental route planning method aimed at minimising risk in Arctic navigation under POLARIS guidance. Sibul et al. (2026) developed a risk-averse routing approach that accounts for uncertainty in sea-ice risk while enforcing a safe speed envelope. More recently, Wang et al. (2026) introduced a multi-objective polar route planning framework based on the NSGA-III algorithm within a POLARIS based risk setting. But the POLARIS still has some limitations because it does not incorporate anthropogenic factors into its risk assessment (Yang et al., 2024). Another line of research has focused on the theory and effectiveness assessment of the POLARIS. The POLARIS solely focuses on sea ice and ship ice-classes as the factors limiting safe navigation for ships (Liu et al., 2024). Therefore, the strategy of implementing speed limits to allow navigation in high-risk areas was considered too risky. The effectiveness of the POLARS in mitigating risks has also attracted the attention of many scholars (Kujala et al., 2019; Stoddard et al., 2016). These studies suggest that the POLARIS provides valuable guidance for ship navigation, however its real-world effectiveness remains unclear, especially when accounting for diverse ship types and operational behaviors.

2.2 Research gaps and contributions

Based on the above critical analysis of the existing relevant literature, the research gaps and contributions are listed below:

(1) Limited large-scale spatio-temporal assessments of POLARIS compliance

191 across ice-classes and ice conditions.

192 Most existing studies are constrained to specific regions, selected ship categories
193 and ice-classes, or short time windows, which prevents a systematic spatio-temporal
194 understanding of POLARIS compliance across different ice-classes and varying ice
195 conditions. Consequently, it remains unclear whether ships of different ice-classes
196 consistently follow the POLARIS risk guidelines and whether the RIO standard
197 effectively supports navigation across diverse ice conditions.

198 Contribution: This study innovatively fuses AIS data with sea-ice datasets,
199 supported by data preprocessing and spatio-temporal correlation methods. POLARIS
200 compliance is then assessed using real-world Arctic shipping traffic (2018–2022)
201 matched with corresponding sea-ice conditions. POLARIS operational effectiveness is
202 quantified by analyzing adherence to and exceedance of its recommended speed limits
203 across a wide range of ship ice-classes.

204 (2) Lack of spatio-temporal characteristics of Arctic shipping traffic under the
205 POLARIS constraints.

206 Prior research has predominantly focused on individual case studies or historical
207 risk assessments, which provides a relatively limited perspective on Arctic navigation
208 risk. Consequently, it remains insufficiently understood how the operational
209 effectiveness of POLARIS is manifested in large-scale spatio-temporal traffic patterns,
210 particularly when compliant and non-compliant operations are explicitly distinguished.

211 Contribution: A spatio-temporal analysis of Arctic shipping traffic is performed in

this study, and patterns in ship speed, trajectories, and risk classification under different ice conditions are identified. Compliant and non-compliant (exceedance) operations are characterized separately, with a particular focus on the spatio-temporal distribution of non-compliance events.

(3) Uncertainty in how the POLARIS accounts for ship-specific operational characteristics

Current implementations of the POLARIS primarily assess risk based on ice conditions, overlooking the impact of ship type and operational behavior on navigation risks. This limitation may lead to inaccurate risk classifications and reduced effectiveness in guiding diverse ship operations in Arctic waters.

Contribution: The impact of different ship types on the effectiveness of the RIO standard under the POLARIS is newly examined in this study, generating policy-making insights to guide its potential modifications and hence improve its real-world applicability.

3. Methodology

In this section, the data used and methodology developed in the study are presented. Firstly, a description of the SIC, Sea Ice Thickness (SIT), and Automatic Identification System (AIS) data is provided, and the preprocessing procedures applied to the AIS data are also described. Subsequently, the POLARIS quantitative sea ice risk model is introduced. In Section 2.3, a spatio-temporal association method is employed to couple sea ice risk with AIS data, and the influence of sea ice on ship navigation is

characterized using a calculation method based on ship traffic characteristics. Finally, the speed restrictions imposed on ships by the POLARIS for different ice-classes are described to assess the effectiveness of the POLARIS.

3.1 Data sources and processing

3.1.1 Data sources

In this study, SIC and SIT data were employed to assess the sea ice conditions at the locations of ice-class ships and to quantify sea ice risk. Therefore, specific requirements for the spatio-temporal resolution of the sea ice data were necessitated. The global ocean data derived from satellite remote sensing, and numerical models are provided by the Copernicus Marine Service (CMS). Its Global Ocean Ensemble Physics Reanalysis dataset (Product ID: GLOBAL_MULTIYEAR_PHY_ENS_001_031) offers homogenized three-dimensional gridded data on the ocean's physical state from 1993 to 2023 (CMEMS, 2024). The dataset contains SIC and SIT data covering the entire world, with a spatio-temporal resolution of 0.25°×0.25°/day. The data is stored in the NetCDF-4 format. Sea ice variables and location information are in a numerical matrix, where each value corresponds to the average value of SIC and SIT at a specific grid cell. Latitude and longitude values denote the center coordinates of each grid cell, and a time series of sea ice data is constructed by overlaying these grids to form three-dimensional representations of SIC and SIT. The SIC variable ranges from 0 (indicating no ice) to 1 (indicating complete coverage), while the SIT variable spans from 0 to 5.5 m, with land areas denoted by NaN.

The AIS is an aid to navigation system that integrates ship identification, tracking, and information exchange to enhance the safety and management of maritime navigation. According to the International Convention for the Safety of Life at Sea (SOLAS), all passenger ships, international cargo ships with a gross tonnage of 300 tons or more and non-international cargo ships with a gross tonnage of 500 tons or more must be equipped with AIS equipment (IMO, 1974). Through the coordinated operation of satellite and shore-based facilities, both static and dynamic ship data are collected and transmitted in real time, thereby recording navigational information (see Table 2).

Table 2. AIS data information

AIS static data			AIS dynamic data		
Variable name	Interpretation	unit	Variable name	Interpretation	unit
MMSI	9-digit ship identification code	-	Time	Ship position timestamp	s
Callsign	Ship call sign	-	Lon	Ship position longitude	°
Name	Ship name	-	Lat	Ship position latitude	°
Type	Ship type	-	Speed	Ship speed	kn
Draught	Ship draught	m	Course	Ship course	°
Length	Ship length	m	Heading	Ship heading	°
Width	Ship width	m	Status	Ship status	-

3.1.2 AIS data preprocessing

Raw AIS data are disturbed by noise, missing values, outliers, and format inconsistencies, all of which can severely affect the accuracy of research findings. To ensure spatio-temporal coherence and reliability, comprehensive preprocessing of AIS data is essential. The data preprocessing steps include cleaning, supplementation, and classification.

The AIS data cleaning includes processing MMSI, heading, ship position, status and speed. The AIS data with non-9-digit MMSI and less than 10 records will be deleted,

and AIS data with heading exceeding 360° will also be removed (Zhou et al., 2023; Ye et al., 2024). Based on the longitude and latitude information in the ship AIS data, entries located over land and islands were identified and discarded. To ensure identification accuracy, coastline data were imported into MATLAB, and the inpolygon function was used to construct a closed polygon from the coastline points. If the location of the AIS data record is inside the polygon, it is determined to be an erroneous record and deleted. The original AIS data also contains the classification of ship status, this study retained only those records corresponding to ships underway. In addition, the data quality can be further improved by identifying and removing abnormal and noise points in the AIS speed data. The AIS data is modeled according to the ship trajectory, and the time T_i, latitude φ_i, longitude λ_i, and speed V_i of the $i-th$ data point of the ship trajectory are described as a track point set S_i.

$$S_i = \left(T_i, \varphi_i, \lambda_i, V_i\right), i = 1, 2, \cdots, N \tag{1}$$

According to the maximum acceleration a_x and maximum deceleration a_m of the ship during navigation, in the time interval ΔT between the trajectory points $[i, i+1]$, the normal ship speed should meet the following conditions:

$$\Delta T = T_{i+1} - T_i \tag{2}$$

$$V_i - a_m \cdot \Delta T \le V_{i+1} \le V_i + a_x \cdot \Delta T \tag{3}$$

After removing the abnormal ship speed, the AIS data still has noise points, mainly including drift points and flying points. This study is based on the ellipse filtering method to construct an ellipse with S_{i-1} and S_{i+1} as the focus. According to the

definition of the ellipse, the product of the maximum navigation speed V_x of the ship and the time interval ΔT_{i-1}^{i+1} is the major axis L. If the ship trajectory point S_i is within the ellipse, the following conditions should be met:

$$L = V_x \times \Delta T_{i-1}^{i+1} \tag{4}$$

$$d\left(S_{i-1}, S_i\right) + d\left(S_i, S_{i+1}\right) \le L \tag{5}$$

where, $d\left(S_i, S_{i+1}\right)$ represents the great circle route distance between the ship track points S_i and S_{i+1}, and R is the average radius of the earth, which is about 6371 km. If the AIS data point does not meet the above conditions, it is considered a noise point and should be deleted.

$$d\left(S_i, S_{i+1}\right) = 2R \cdot \arctan\left(\sqrt{\frac{h\left(S_i, S_{i+1}\right)}{1-h\left(S_i, S_{i+1}\right)}}\right) \tag{6}$$

$$h\left(S_i, S_{i+1}\right) = \sin^2\left(\frac{\varphi_{i+1}-\varphi_i}{2}\right) + \cos\left(\varphi_{i+1}\right)\cos\left(\varphi_i\right)\sin^2\left(\frac{\lambda_{i+1}-\lambda_i}{2}\right) \tag{7}$$

In the raw AIS data, ship type information is disturbed by inconsistent formatting and missing entries. By linking MMSI with the Lloyd's Register Archive, ship type information was verified, supplemented, and standardized. In this study, the supplemented ship type data were reclassified into Cargo, Tanker, Passenger, Fishing, and Other. Cargo includes Bulk carriers, General Cargo ships, Liquid Cargo ships, LPG carriers, LNG carriers, and Container ships. Tankers include Chemical tankers and Oil tankers. Passenger includes Passenger Cruise Ship and Passenger Ferry Ship. Fishing includes Fishing ships. Other includes Yacht, Tugs, Ro-Ro Ships, Ro-Ro Cargo, Naval/Government ships, Training ships, Icebreakers, Research vessels, Sailing vessels, Marine engineering ships, Supply/Support Service vessels, Fuel Supply vessels, Pilot

vessel and Undefine.

The raw AIS data does not include ship ice-class information. To address this limitation, the ship ice-class certificate recorded in the Lloyd's Register Archive was queried based on MMSI to complete the supplement of ice-class information in the AIS data. This study uses the ship ice-class classified by the POLARIS, which ranks from the highest (PC1) to the lowest (IC), and associates the ice-class attributes of the ship in the raw AIS data. Then, ships were categorized based on their respective ice-classes.

3.2 Quantification of sea ice risk

The POLARIS-based RIV classification for ships of different ice-classes across various SIT ranges is presented in Table 3, which illustrates the correspondence among sea ice type, SIT, and RIV.

Table 3. Risk index values (IMO, 2016).

Ice-class	Ice-Free	New Ice	Grey Ice	Grey White Ice	Thin First Year Ice 1st Stage	Thin First Year Ice 2nd Stage	Medium First Year	Medium First Year Ice	Thick First Year Ice	Second Year Ice	Light Multi Year Ice	Heavy Multi Year Ice
SIT (m)	0	(0, 0.1]	(0.1, 0.15]	(0.15, 0.3]	(0.3, 0.5]	(0.5, 0.7]	(0.7,95]	(0.95, 1.2]	(1.2, 2]	(1.2, 2]	(2, 2.5]	>2.5
PC1	3	3	3	3	2	2	2	2	2	2	1	1
PC2	3	3	3	3	2	2	2	2	2	1	1	0
PC3	3	3	3	3	2	2	2	2	2	1	0	-1
PC4	3	3	3	3	2	2	2	2	1	0	-1	-2
PC5	3	3	3	3	2	2	1	1	0	-1	-2	-2
PC6	3	2	2	2	2	1	1	0	-1	-2	-3	-3
PC7	3	2	2	2	1	1	0	-1	-2	-3	-3	-3
IA Super	3	2	2	2	2	1	0	-1	-2	-3	-4	-4
IA	3	2	2	2	1	0	-1	-2	-3	-4	-5	-5
IB	3	2	2	1	0	-1	-2	-3	-4	-5	-6	-6
IC	3	2	1	0	-1	-2	-3	-4	-5	-6	-7	-8
Open Water	3	1	0	-1	-2	-3	-4	-5	-6	-7	-8	-8

The formula for calculating the RIO provided by the POLARIS is as follows:

$$RIO = \sum (C_1 \times RIV_1) + (C_2 \times RIV_2) + (C_3 \times RIV_3) + ... + (C_n \times RIV_n) \quad (8)$$

where RIO denotes the POLARIS-quantified sea ice risk index outcome, $C_1, \ldots, C_n$ indicates the SIC that is distributed at various locations within the navigational waters expressed in decimal units and extracted from the sea-ice dataset described in Section 3.1.1, and $RIV_1, ..., RIV_n$ represents the risk values derived from converting the SIT at the corresponding positions. It is worth noting that the larger the RIO value, the safer the ship's navigation. Conversely, the smaller the RIO value, the higher the navigation risk.

3.3 Ship speed characteristic measurement

Based on AIS data, the distribution characteristics of ship speeds across different sea areas were analyzed. To ensure an accurate representation of ship speeds, the AIS coverage area was partitioned into grids of 0.1°×0.1°.

The ship speed assigned to each grid cell is not computed as the mean of all AIS speed points within the cell. Instead, it is calculated by averaging the per-ship mean speeds within that cell (Wang et al., 2020). For each grid cell, the mean speed is first calculated separately for every ship that enters the cell by averaging that ship's AIS speed points recorded within the cell. The grid cell speed is then obtained by averaging these per ship mean speeds across all ships that entered the cell. This approach prevents ships with dense AIS sampling from unduly influencing the grid cell mean, resulting in a spatial distribution of ship speeds that is more representative of typical traffic level operating conditions. The calculation formula of the ship speed $\overline{V}$ of the unit grid is as follows:

$$\overline{V} = \frac{1}{M}\sum_{j=1}^{M}\overline{V_j} \tag{9}$$

$$\overline{V_j} = \frac{1}{\left|S_{A,j}\right|}\sum_{(T_i,\varphi_i,\lambda_i,V_i)\in S_{A,j}} V_i,\ j = 1,2,\cdots,M \tag{10}$$

$$S_A = \bigcup_{j=1}^{M} S_{A,j}, S_{A,j} \cap S_{A,k} = \varnothing\left(j \neq k\right) \tag{11}$$

$$S_A = \left\{\left(T_i,\varphi_i,\lambda_i,V_i\right) \in S \mid \left(\varphi_i,\lambda_i\right) \in G_A\right\} \tag{12}$$

where $\overline{V_j}$ represents the average speed of the j-th ship in the unit grid, and M represents the total number of ships. Additionally, S_A is the set of all ship trajectory

points in the calculated unit grid G_A, and $S_{A,j}$ represents the set of trajectory points corresponding to the j-th ship, divided according to MMSI.

The above-described method is used to depict the spatio-temporal distribution of shipping traffic characteristics, as shown in Figs. 4 and 5.

3.4 Spatio-temporal correlation between ships and sea ice

Since sea ice data and AIS data have different storage formats and update frequencies, it is necessary to perform spatiotemporal correlation between the two types of data.

The nearest-neighbor search algorithm is used in this study to query and associate sea ice conditions with the location of each AIS data point, this approach can better illustrate the influence of sea ice on ship navigation behavior (Liu et al., 2025; Shu et al., 2025). The process of associating ships with sea ice is as follows: Firstly, the timestamp T_i recorded in the AIS data is converted into the corresponding day of the year. Secondly, the great-circle route distance between the ship trajectory points and the center points of each sea ice grid is calculated and the grid index position with the minimum distance is found. Finally, the SIC and SIT data for that grid cell on that day are retrieved, establishing a spatiotemporal association. The sea ice dataset Ice contains the latitude φ_g, longitude λ_g, time T_g of the g-th grid position in the sea ice grid, as well as the SIC_g and SIT_g. The definition is as follows:

$$Ice = \left\{ Ice_g = \left(\varphi_g, \lambda_g, T_g, SIC_g, SIT_g \right) \mid g = 1, 2, \cdots, K \right\} \tag{13}$$

$$day_i = \left\lfloor \frac{T_i - T_{Jan1}}{T_s} \right\rfloor + 1 \tag{14}$$

where timestamp T_i in the AIS data is accurate to the second, the T_{Jan1} represents the timestamp of 0:00 on January 1 of that year, and T_s represents the total number of seconds in a day, which is 86,400. The AIS data time is converted by using the floor function $\lfloor \cdot \rfloor$, and the day_i of the year when the AIS data timestamp is found. The distance between the ship trajectory points $S_i(\varphi_i, \lambda_i)$ and the center of the grid point $Ice_g(\varphi_g, \lambda_g)$ is calculated as $d(S_i, Ice_g)$. Then, calculate the great-circle route distance between the ship trajectory point $S_i(\varphi_i, \lambda_i)$ and all grid center points, and find the sea ice grid with the smallest distance to the ship trajectory point. $D_{index}(\cdot)$ is the query grid linear index function, and each ship trajectory point $S_i(\varphi_i, \lambda_i)$ defines its grid point linear index position $j^*(S_i)$ as:

$$j^*(S_i) = D_{index}\left(\arg\min_{g=1,2,\cdots,K} d(S_i, Ice_g)\right) \tag{15}$$

where $\arg\min f(x)$ denotes the variable x that makes the function $f(x)$ achieve the minimum value in the set X, that is the independent variable that makes the objective function reach the extreme value. Therefore, according to the conversion time day_i of the ship trajectory point $S_i(\varphi_i, \lambda_i)$ and the linear index $j^*(S_i)$ position, the SIC_i and SIT_i can be queried, and the associated mathematical model is:

$$SIC_i = SIC(day_i, j^*(S_i)) \tag{16}$$

$$SIT_i = SIT(day_i, j^*(S_i)) \tag{17}$$

The above-described method is used to analyse the relationship between ship speed and sea ice risk, as shown in Figs. 6 and 7, and to derive the subsequent non-compliance indicators.

3.5 Effective assessment of the POLARIS

Based on the differing sea ice tolerance capacities of ice-class ships, the elevated operational guidelines for navigation within distinct RIO intervals have been delineated by the POLARIS (see Table 4). Three sea ice navigation risk levels are divided, with the RIO of 0 and -10 as the boundaries. As the RIO decreases, for PC1-PC7 ice-class ships, the three levels are normal operation, elevated operational risk, and operation subject to special consideration. In contrast, due to their markedly reduced ice-breaking capabilities, ships with ice-classes lower than PC7 do not exhibit an elevated operational risk level but are directly classified as operation subject to special consideration.

Table 4. Risk index outcome Criteria (IMO, 2016).

RIO_{SHIP}	Ice-classes PC1-PC7	Ice-classes below PC7 and ships not assigned an ice-class
RIO≥0	Normal operation	Normal operation
-10≤RIO<0	Elevated operational risk	Operation subject to special consideration
RIO<-10	Operation subject to special consideration	Operation subject to special consideration

The POLARIS provides recommended operational measures for ships entering Elevated operational risk waters, which include increased vigilance, the use of icebreaker assistance, and speed reduction. In this study, Elevated operational risk waters (-10≤RIO<0) are hereafter referred to as the high-risk range. If speed reduction is adopted as the operational measure, the POLARIS provides guidance on speed limits for different ice-class ships (see Table 5). When ships sail at reduced speed in waters with elevated operational risk, the speed should not exceed the recommended speed limit standard given by the POLARIS. Moreover, when the ships enter operation subject

to special consideration waters, the captain and senior crew on navigation duty must exercise heightened caution. In addition, ship operators should take operational actions to reduce the risk to the ship, including altering course, further reducing speed, and applying other special interventions to lower navigational risks. Therefore, ships are classified as non-compliance if they exceed the recommended speed limits within the high-risk range or enter waters where operations are subject to special consideration.

Table 5. Recommend speed limits for elevated risk operations (IMO, 2016).

Ice-Class	Recommended Speed Limit
PC1	11 knots
PC2	8 knots
PC3-PC5	5 knots
Below PC5	3 knots

The recommended speed limits proposed by POLARIS for different ice-class ships within the high-risk range were used as the compliance benchmark. Exceedance frequency and exceedance magnitude were adopted as quantitative indicators to assess the POLARIS effectiveness.

The exceedance magnitude ΔV_k is defined as the amount by which the observed speed exceeds the recommended speed limit by the POLARIS. The definition is as follows:

$$\Delta V_K = V_{obs,k} - V_{rec,k} \tag{18}$$

Where $V_{obs,k}$ denotes the observed speed at AIS record k, and $V_{rec,k}$ denotes the corresponding recommended speed limit derived from Table 5. Only record with $\Delta V_k > 0$ are treated as exceedance events. The exceedance frequency E is used to quantify how often ship speeds exceed the POLARIS recommended speed limits, and

is defined as follows:

$$E = \frac{1}{|\Omega|} \sum_{k \in \Omega} I_k \tag{19}$$

Where Ω denotes the set of AIS records included in the evaluation, and the I_k is the exceedance indicator for AIS record k.

In order to eliminate the impact of idling and drifting ship recording points on the statistical results of ship navigation behavior in ice-covered areas, a speed threshold of 1 knot is applied to exclude these situations (Zhou et al., 2018; Similä and Lensu, 2018). Similarly, record points where the SIC is below 0.15 or the SIT is below 0.1 m are excluded to mitigate the influence of weak ice on ship navigation behavior (Wang et al., 2021). Subsequently, based on the spatio-temporal association between the AIS data from different ice-classes ships and the sea ice data, the effect of the RIO on ship speed is quantified. The speeds of ice-class ships across different RIO intervals are then compared with the recommended speed limits to assess the adherence to the POLARIS under actual operating conditions. For ships that do not comply with the POLARIS, the spatio-temporal distribution of non-compliance rates and non-compliance behaviors is further analyzed.

4. Experimental results and deep analysis

In this section, the RIO of different ice-class ships in each SIC and SIT interval is first quantified based on the POLARIS risk calculation framework, and the spatio-temporal distributions of RIO encountered by PC3 ice-class ships are exhibited.

Subsequently, the navigational speeds of ships of different ice-classes were displayed and spatio-temporally correlated with the RIO. Afterwards, ship non-compliance in high-risk areas were counted. For compliant ships, the effect of the RIO on the speed of different types of ships was further explored. Finally, regions and time periods with high-incidence of non-compliance were identified and presented to assess the effectiveness of the POLARIS. The research area consists of six major seas from east to west, including the Norwegian Sea, the Barents Sea, the Kara Sea, the Laptev Sea, the East Siberian Sea, and the Chukchi Sea, as shown in Fig. 1.

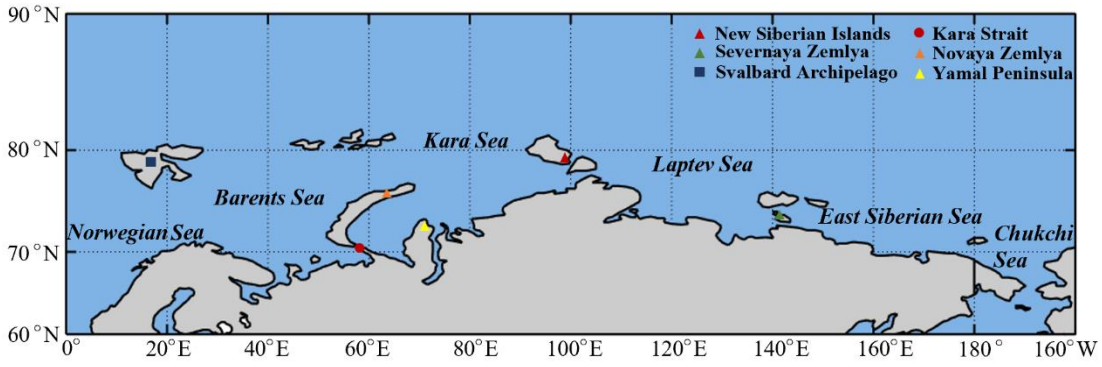

Fig. 1. Map of the research area. (The key seas and straits along the area).

Arctic sea ice data and AIS data from 2018 to 2022 were used to study the effectiveness of the POLARIS. Based on the AIS data preprocessing in Section 2.1.2, a total of 6,366 missing ship type entries were supplemented from Lloyd's Register Archive. According to the Polar Code, ships operating in the ice-covered polar waters are required to adhere to the designated Polar Class (PC) or an equivalent ice-class standard to ensure compliance and safety. In this study, ships with ice strengthening are referred to as ice-class ships. Of the 30,484 ships on Arctic voyages collected over five years, only 5,650 ships were found to have records of the Ice Class Certificate published

by the International Association of Classification Societies (IACS) and ship ice-classes designated by the Finnish-Swedish Ice Class Rules (FSICR). These ships, which span ice-classes from PC2 to 1C in descending order across a total of 10 levels, were used to analyse the characteristics of Arctic shipping traffic. For the POLARIS effectiveness assessment, however, analysis was restricted to the subset of ice-class ships that actually operated in ice-covered waters, as summarised in Table 6.

Table 6. Ice-class ships of the POLARIS effectiveness assessment dataset

Ship ice-class	PC2	PC3	PC4	PC5	PC6
Number of ships	2	24	18	6	25
Number of AIS records	148034	6,436,967	3,159,885	648,825	649,115
Ship ice-class	PC7	IA Super	IA	IB	IC
Number of ships	11	34	187	182	557
Number of AIS records	635,069	91,279	168,141	258087	130230

4.1 Sea ice risk distribution

According to the sea ice risk calculation rules of the POLARIS, the influence of SIC and SIT on the RIO values of ships of various ice-classes is quantified, as shown in Fig. 2. For PC2 ice-class ships, the minimum RIO value is 0 when the SIC reaches 100% and the SIT exceeds 2.5 m, which means that the ship will always be within safe limits when navigating the Arctic's main shipping routes. As the ship ice-class gradually decreases, the high-risk area begins to expand negatively and gradually emerges towards high-SIC and high-SIT areas. Notably, risk boundaries shift along both SIC and SIT, underscoring the joint dependence of RIO on SIC and SIT. For lower ice-class ships, RIO shows greater sensitivity to variations in SIC and SIT, such that comparable changes in sea ice conditions produce larger changes in RIO than for higher ice-class

ships. Overall, the RIO calculation framework provided by the POLARIS reveals a complex interplay among ship ice-class, SIC, and SIT.

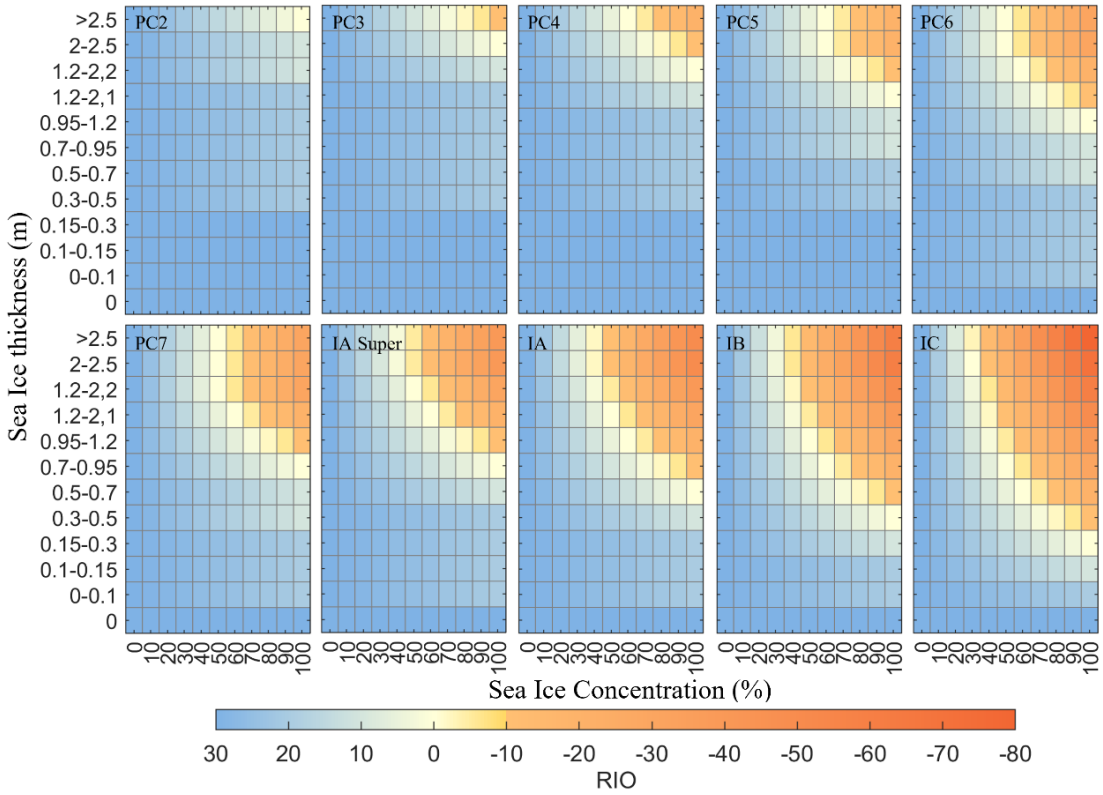

Fig. 2. Quantification of the RIO and data point statistics for each ice-class ship.

The sea ice risk for PC6 ships in the study area is quantified month by month in Fig. 3. As can be seen, the sea ice risk has significant monthly variation characteristics. From January to May, due to continued low temperatures and continuous accumulation of sea ice, the sea ice risk in the region increased month by month, peaking in May. During this period, high-risk areas and those requiring special operational measures are primarily located in key navigational water bodies, such as the East Siberian Sea, the Vilkitsky Strait, and the Sannikov Strait, which pose significant threats to ship safety. Since June, as temperatures gradually rise and sea ice melt accelerates, the region's sea ice risk noticeably diminishes, reaching its annual minimum in September. Thereafter,

503 a renewed escalation of sea ice risk was induced by a decline in temperature from
504 October to year-end, with the eastern waters of the Yamal Peninsula increasingly
505 covered by sea ice, further aggravating the risk conditions.

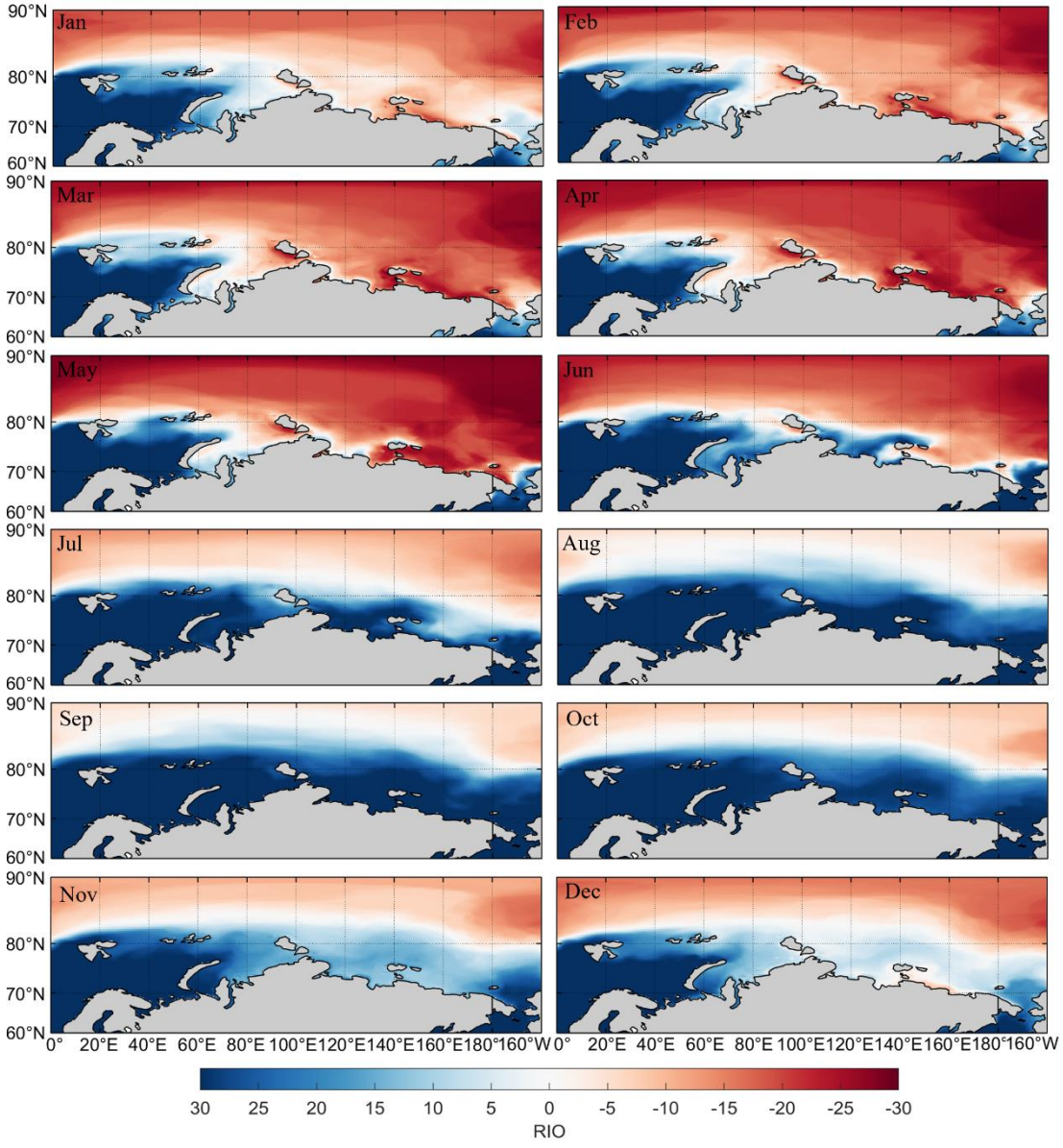

506
507 Fig. 3. Spatio-temporal distribution of sea ice risk for PC6 ice-class ships.

508 From a spatial perspective, only the coastal areas of the Norwegian Sea and the
509 Barents Sea remain ice-free throughout the year. The 80°N latitude line delineates a
510 clear boundary in sea ice risk, with navigational hazards increasing significantly with
511 latitude. Moreover, the East Siberian Sea is characterized by complex sea ice conditions

and an uneven distribution of ice thickness. The formation of dense pressure ridges and thick ice regions—driven by the combined influence of ocean currents and wind—poses a great threat to navigation safety. The Vilkitsky Strait is a narrow channel between several key sea areas. Its special terrain makes it easy for ice to accumulate. Even when the ice conditions ease in the summer, it remains a high-risk zone requiring special attention.

4.2 Spatio-temporal distribution of ship speed

The speed distribution of Arctic ship traffic under varying ice conditions reveals pronounced disparities across ice-class categories (Fig. 4). Generally, as the ice-class decreases, a clear decline in navigational speed is observed, accompanied by a progressive contraction in the latitudinal extent of navigable waters. High ice-class ships, such as those classified as PC2 and PC3, sustain higher speeds across broader regions, particularly below 80°N. In contrast, lower ice-class ships exhibit a marked reduction in speed as they approach higher latitudes, underscoring the substantial constraints imposed by the Arctic's harsh ice conditions. Spatially, the distribution of ship trajectories is notably uneven: ship density is highest in the Norwegian and Barents Seas to the west and tapers off toward the Laptev, East Siberian, and Chukchi Seas in the east—mirroring the increasing severity of sea ice in that direction. The performance gap between ice-classes is also evident. PC2 ice-class ships typically maintain speeds above 12 knots below 80°N, declining to approximately 10 knots at higher latitudes. PC3-class ships, however, preserve speeds exceeding 12 knots across most regions,

highlighting their superior ice-capable design. For ships rated below PC7, speeds are generally clustered between 10 and 12 knots, with operations largely confined to the nearshore waters west of Svalbard. These patterns underscore the importance of ship ice-class and spatial variability in sea ice conditions in shaping Arctic navigability. In this extreme environment, both structural capability and geographic distribution of ice severity critically influence the operational performance and safety of polar shipping.

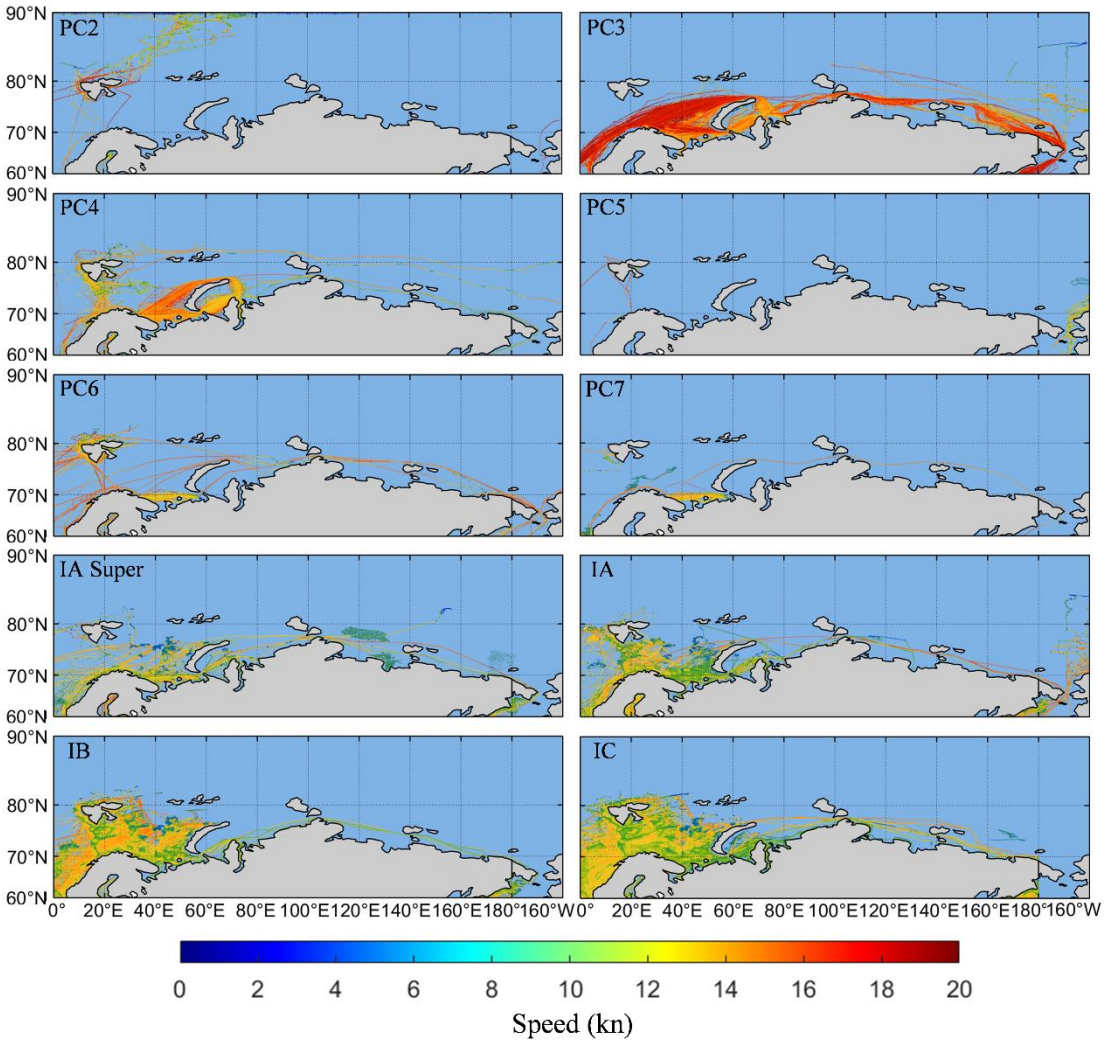

Fig. 4. Distribution of navigation characteristics of different ice-classes ships.

In order to fully study the impact of seasonal changes on ships, the PC3 ice-class ships are taken as an example and its speed distribution diagram is plotted month by

543 month in Fig. 5. The navigation characteristics of ships in the Arctic areas show a
544 significant correspondence with the seasonal changes in sea ice risk.

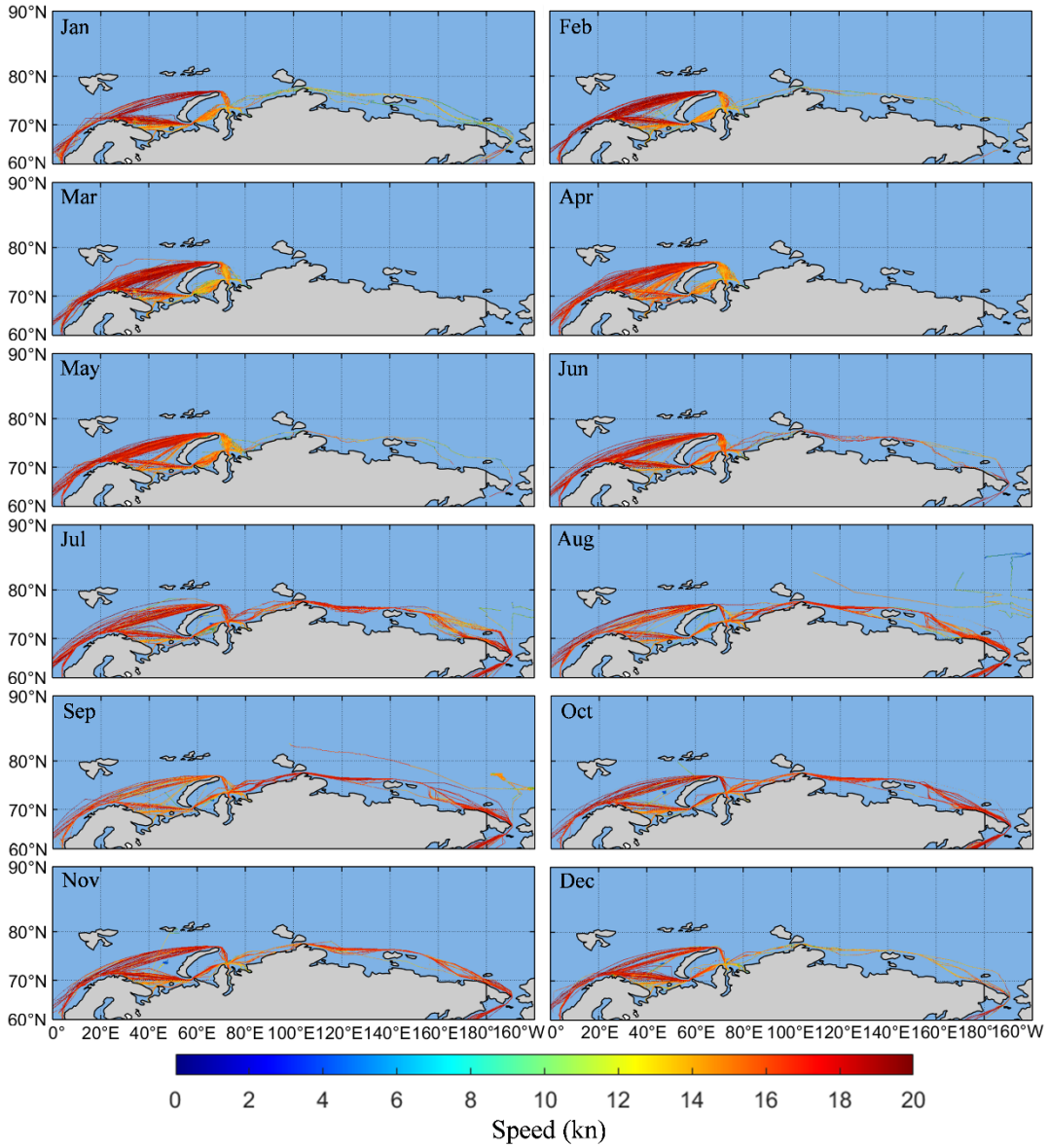

545
546 Fig. 5. Spatio-temporal distribution of navigation characteristics of PC3 ice-class ships

547 In the ice-free waters west of the Kara Strait, shipping activities are relatively
548 dense year-round, with overall navigational speeds maintained at approximately 16
549 knots. During March and April, when the sea ice risk was severe, there was almost no
550 transiting navigation in the Arctic. The ship speed in the Kara Sea between the northern
551 part of Novaya Zemlya and the Yamal Peninsula slows down to a speed between 12 and

552 14 knots. In May, although trans-Arctic trajectories began to emerge, the sea ice risk
553 remains at its annual peak, and ship speeds show little improvement. By July and
554 August, as the sea ice risk rapidly diminishes, transit speeds reach their highest levels
555 for the year. Notably, although sea ice risk reaches its minimum in September, both ship
556 speeds and the number of trajectories begin to decline approximately one month earlier.
557 This observation suggests that although Arctic shipping characteristics are strongly tied
558 to seasonal sea ice variations, shipping schedules are not strictly aligned with the period
559 of optimal ice conditions. Rather, operational and commercial demands may advance
560 the peak in maritime activity relative to the period of minimal sea ice risk.

561 **4.3 Assessment of the POLARIS effectiveness**

562 In this section, firstly, the compliance of each ice-class ships with the POLARIS
563 in actual navigation and the fitting relationship between speed and RIO were assessed
564 respectively. Secondly, for compliant ships, the influence of ship type on navigation
565 risk and ship speed was studied. Finally, for non-compliant ships, the areas with a high-
566 incidence of non-compliance and navigation time were quantified. In summary, the
567 effectiveness of the POLARIS in guiding actual ship navigation was assessed.

568 4.3.1 Ship compliance with the POLARIS

569 In Fig. 6, each panel corresponds to a single ship ice-class and is based on all ships
570 belonging to that class. The relationship between speed and the RIO for each ice-class
571 ships is summarised by binning observations into 1-unit RIO intervals. Each blue point
572 in the figure represents the mean speed of ships in that ice-class within the

corresponding RIO bin. The slopes of the linear fitting fits are uniformly negative, indicating a clear trend of decreasing ship speed with increasing RIO for each ice-class, as revealed by the analysis of ships with ice-classes PC2-PC7 and IA (see Fig. 6). However, the RIO data points for ships with ice-classes IA Super-IB were relatively sparse and primarily confined to the safe range. Consequently, the differences in the number of data points across the ranges undermine the overall significance of the fit.

In addition, except for PC4, the RIO values for PC2–PC5 ice-class ships remain within the safe range. As ice-class decreases, the lower bound of the RIO values progressively declines. When the ice-class drops to PC6 and below, the minimum RIO falls within the range requiring special operations, indicating that low ice-class ships may operate in high-risk conditions during real-world navigation. Notably, when PC7 ice-class ships operate in the range requiring special operations, their mean speed does not immediately decrease to within the recommended speed limits. For example, when RIO was between −13 and −12, the mean speed of PC7 ice-class ships was 9.21 kn. The mean speed did not fall below 3 kn until RIO decreased further, to approximately below −16. This pattern suggests that, even when risk reaches levels necessitating special operations, some operations may not fully reflect the speed reduction and other precautionary measures recommended by POLARIS guidance.

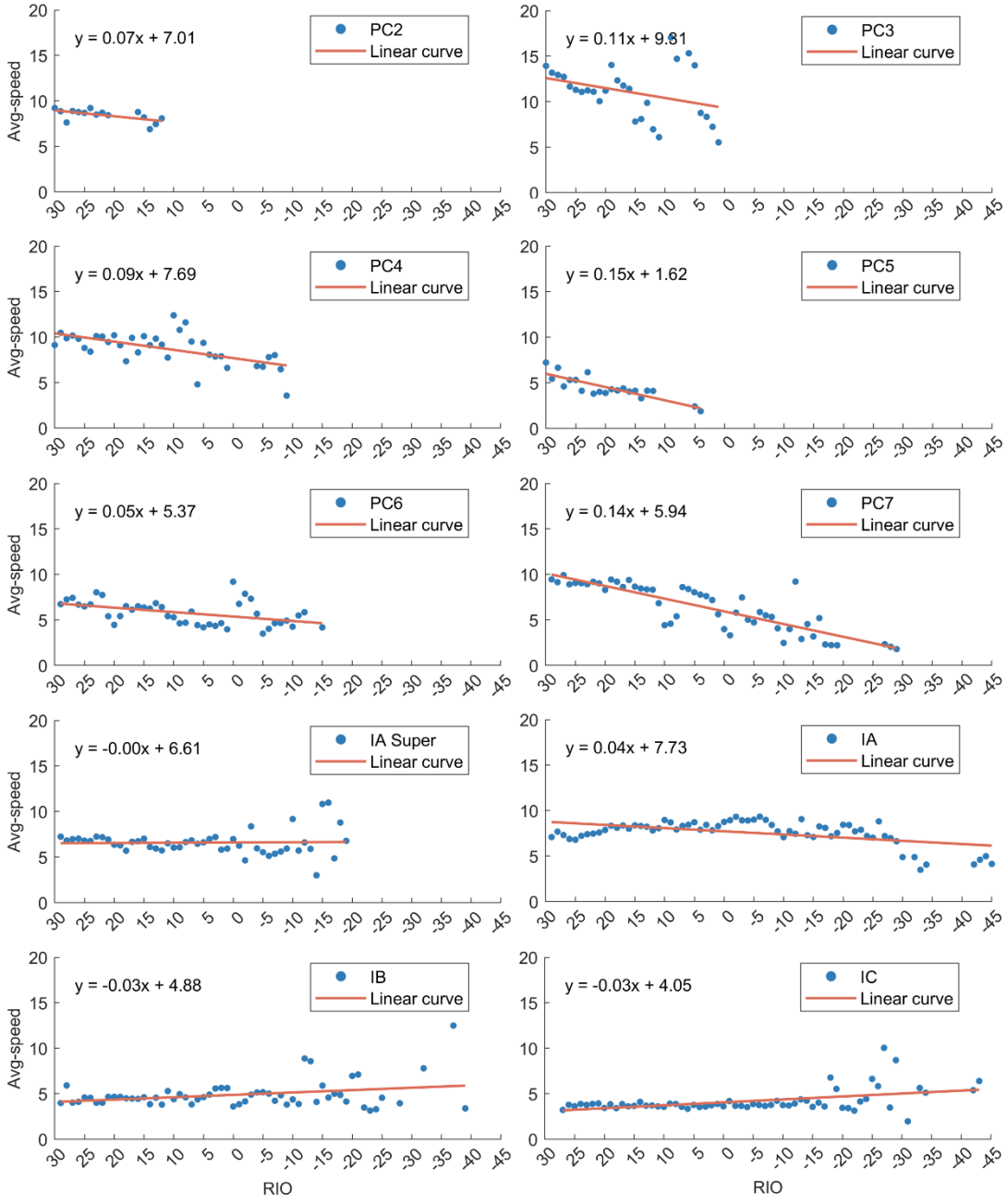

Fig. 6. Relationship between speed and the RIO for each ship ice-class.

In the high-risk intervals, PC4 ice-class ships operating at speeds exceeding 5 knots, PC6 and PC7 ice-classes ships exceeding 3 knots are classified as non-compliant. The Non-compliance rates for each consecutive RIO interval, as well as the overall rate in the high-risk area, are summarized in Table 7. Although the overall non-compliance rates of the three ice-classes ships are similar, namely 68.21%, 70%, and 66.18%,

598 respectively, pronounced differences are observed across individual RIO intervals.
599 Specifically, non-compliance among PC4 ice-class ships is concentrated in extremely
600 high-risk intervals such as [-7, −6) and [-6, −5), where the non-compliance rate
601 approaches 80%. When the risk is reduced, the non-compliance will decrease rapidly
602 or even disappear. In contrast, PC6 ice-class ships show more frequent non-compliance
603 in the RIO intervals close to safety criticality, such as [-4, -3), [-2, -1), and [-1, 0), with
604 a non-compliance rate close to or reaching 100%. PC7 ice-class ships had a higher non-
605 compliance rate in the medium risk interval and showed a fluctuating downward trend
606 as the risk increased further. In summary, the non-compliance rate will increase at the
607 head and tail boundaries of the high-risk intervals, while the non-compliance rate in the
608 middle intervals will be relatively reduced. It is demonstrated by the above research
609 results that effective guidance and supervision measures for ship behavior are provided
610 by the POLARIS.

611 Table 7. Non-compliance to POLARIS speed guidance in high-risk RIO intervals: exceedance
612 frequency (%).

Ice-class (RIO)	[-10,-9)	[-9, -8)	[-8, -7)	[-7, -6)	[-6, -5)	[5, -4)	[-4, -3)	[3, -2)	[-2, -1)	[-1, 0)	Total
PC4	18.67	59.27	75.09	80.00	80.66	75.00	-	-	-	-	68.21
PC6	79.05	62.79	44.44	54.69	47.50	50.00	100	96.00	88.46	100	70.00
PC7	53.10	71.54	71.94	77.37	58.69	66.46	90.70	74.55	31.43	46.15	66.18

613 The median exceedance magnitude for non-compliance with POLARIS speed
614 guidance across high-risk intervals is reported in Table 8. Consistent with the overall
615 pattern for exceedance frequency, the largest median exceedance magnitude is
616 exhibited by PC6 ice-class ships, reaching 3.55 kn. It is followed by PC7 ice-class ships,

617 at 3.30 kn, and PC4 ice-class ships, at 2.90 kn. PC6 maintains relatively high
618 exceedance magnitudes across multiple bins as RIO moves from [-5, −4) towards the
619 safety criticality, and peaks at 6.25 kn in [-5, −4) and 6.30 kn in [-3, −2). For PC7 ice-
620 class ships, a clear peak of 5.10 kn occurs in [-4, −3), followed by a decrease to 2.25 kn
621 as RIO approaches [-1, 0). Across intervals, the median exceedance magnitude for PC4
622 ice-class ships increases from 1.80 kn in [-10, −9) to 4.00 kn in [-8, −7), and then
623 gradually declines, falling to 1.85 kn in [-5, −4). The high exceedance frequency and
624 substantial exceedance magnitude observed in the high-risk range suggest that
625 POLARIS navigational recommendations may require further refinement to better
626 reflect real-world maritime operations.

627 Table 8. Non- compliance to POLARIS speed guidance in high-risk RIO intervals: median
628 exceedance magnitude (kn).

Ice-class (RIO)	[-10,-9)	[-9, -8)	[-8, -7)	[-7, -6)	[-6, -5)	[5, -4)	[-4, -3)	[3, -2)	[-2, -1)	[-1, 0)	Total
PC4	1.80	3.10	4.00	3.40	2.20	1.85	-	-	-	-	2.90
PC6	2.30	2.35	4.95	3.10	1.90	6.25	4.15	6.30	4.55	5.9	3.55
PC7	2.35	3.30	3.60	4.00	3.40	3.20	5.10	4.00	3.20	2.25	3.30

629 Icebreaker escort can increase operating speeds, and therefore interpretations
630 based on exceedance criteria may be confounded. Owing to limited data, we compiled
631 16 icebreaker-led convoy cases and analysed the following ships in each convoy. The
632 escort subset comprised nine PC4 ice-class ships, four PC6 ice-class ships, and three
633 PC7 ice-class ships. After spatio-temporal matching with the sea ice risk field, all PC4
634 ice-class ships escort records remained within the safe regime. Most PC6 ice-class ships
635 escort samples did not operate in ice-covered waters. Only one PC7 ice-class ship

briefly entered the high-risk and special-operation regimes. For this ship, 4,067 convoy-following AIS points were identified, of which 17 (0.42%) occurred in the high-risk regime and 20 (0.49%) in the range requiring special operations, with a minimum RIO of −14.11. According to POLARIS, when planning a voyage after deciding to use an icebreaker escort, the risk index result derived from historical ice data not under escort can be assumed to be the calculated value plus 10, however the RIO under escort should not be adjusted using an additional correction term in practice (IMO, 2016). Even after this adjustment, the mean speed within the high-risk regime remained 9.15 kn, exceeding the recommended speed guidance. Therefore, under the current data availability, icebreaker escort is therefore unlikely to materially bias the traffic-scale statistics reported here.

4.3.2 Factors influencing Risk

The compliant ships under each ice-class were screened out and differentiated by ship type to study the influence of ship type on the relationship between ship speed and RIO, as shown in Fig. 7. The speeds of various types of ships vary significantly under different ice-class conditions.

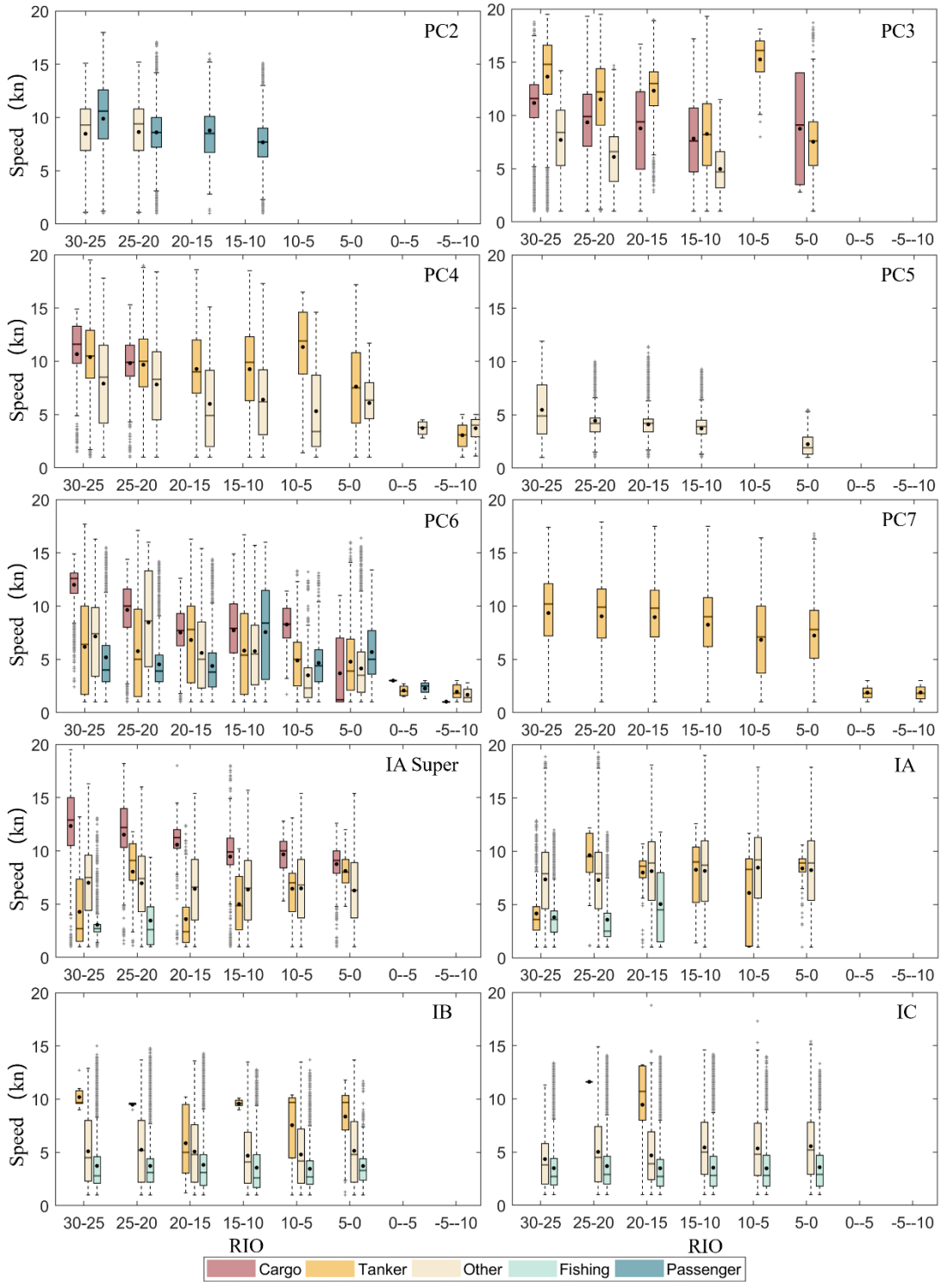

Fig. 7. Impact of RIO on speed of different ship types in compliant ships

Overall, Cargo ships and Tankers typically maintain higher speeds, followed by passenger ships, while the speeds of Other and Fishing ships are relatively low. It is worth noting that, except for Fishing, all ship types are distributed in PC6 ice-class,

657 which is the ice-class with the most abundant ship types, while Fishing ships are mainly
658 distributed among low ice-class ships of PC7 and below. In addition, as the ice-class of
659 the ship decreases, the average speed of the same ship type in the same RIO interval
660 shows a gradual downward trend. For example, when the Tanker under PC3 ice-class
661 is in the RIO interval of (30–25), the average speed of the Tanker can reach 13.64 knots,
662 while it drops to 10.39 knots in the same interval under PC4 ice-class. This study also
663 found that speed disparities among various ship types were more pronounced in higher
664 RIO ranges, but these differences gradually diminished as the RIO values decreased.
665 This shows that in harsh sea ice conditions, the physical properties of various types of
666 ships will be restricted. Therefore, in addition to considering sea ice conditions and ship
667 ice-classes, it is necessary to pay attention to the key role of ship type in determining
668 speed and risk level.

669 4.3.3 High-incident regions and periods of non-compliance

670 The high-incidence areas of non-compliance events for each ice-class are
671 quantified in Fig. 8. In general, as the ice-class of ships decreases, there is a marked
672 increase in the number of non-compliant ships, non-compliance trajectory points, and
673 the extent of clustered regions. The Kara Strait was the area with the highest incidence
674 of non-compliance, with all seven ice-classes ships recording instances of non-
675 compliance. Additionally, non-compliance events have been observed for PC4, PC6,
676 IB, and IC ice-classes ships in the waters near the northwestern region of the Svalbard
677 Archipelago, around 80°N. In addition, the Kara Sea between the northern part of

Novaya Zemlya and the Yamal Peninsula also requires special attention. In this area, except for PC6 and PC7 ice-classes ships, all other ice-classes ships have records of non-compliance trajectories. The areas with high-incidence of these non-compliance events are highly spatially corresponding with the distribution of sea ice risks. For example, the waters near the Svalbard Islands and the Kara Strait are both critical waters of high-risk areas during severe sea ice months. The remaining non-compliance areas are mainly concentrated in the waters east of the Kara Strait, which are threatened by sea ice all year round. This further confirms the impact of geographical and spatial differences on ship navigation safety.

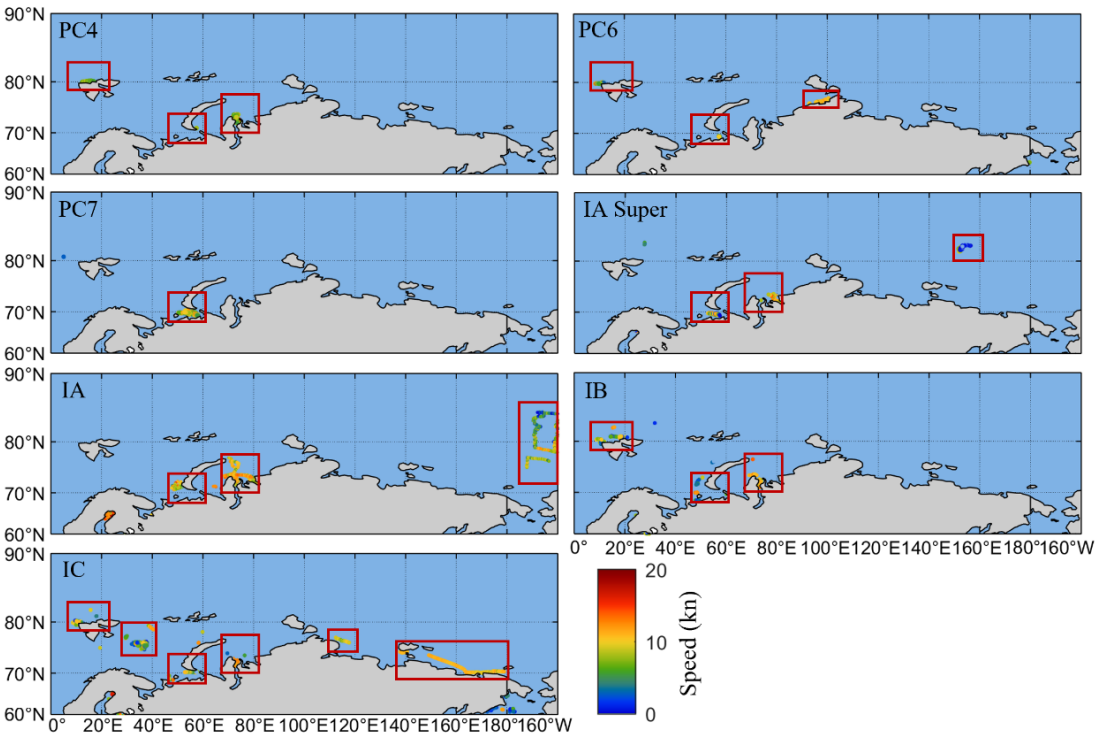

Fig. 8. Distribution of Non-Compliant ship navigation areas.

The navigation time of the non-compliant ships throughout the year is quantified in Fig. 9. The temporal distribution of non-compliance among ships of different ice-classes exhibits pronounced seasonal variations that are closely linked to sea ice risk in

the Arctic. Winter and spring (January to June) are the main concentrated times for non-compliance, especially from April to June, when the sea ice risk is the highest. However, certain ice-classes ships exhibit almost no non-compliance during July to October, the period with the mildest ice conditions of the year. These findings underscore the increased sensitivity of lower ice-classes ships to fluctuations in sea ice risk. In future Arctic shipping management, special attention should be paid to the navigation behavior of low-ice-class ships during severe sea ice seasons.

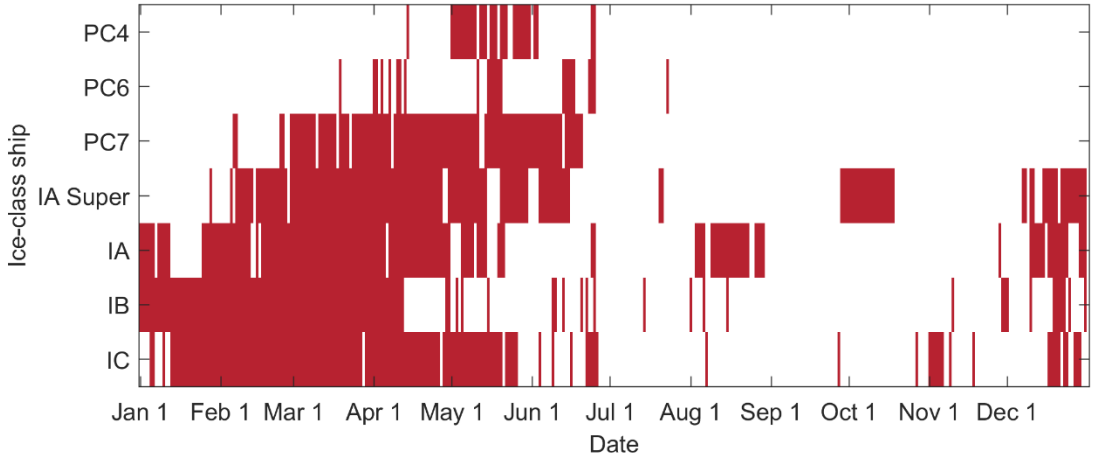

Fig. 9. Distribution of Non-Compliant ship navigation periods.

5. Discussion and implications

Polar rescue will be more challenging than in other traditional waters once a navigation hazard occurs due to the complex ice navigation environment and the unique geographical location (Chen et al., 2025). Consequently, to ensure navigational safety, ships operating in Arctic ice-covered areas must rigorously adhere to polar navigation rules. The POLARIS is widely recognized as an effective tool for mitigating navigation risks in ice-covered waters and is extensively employed in polar ship navigation. The navigation risks of ships of different ice-classes under various SIC and SIT are

quantified by the POLARIS. The system also provides ships with corresponding risk level classifications, recommended restricted navigation speeds, and sea ice risk thresholds for restricted navigation waters. Nevertheless, whether Arctic ships truly follow the navigational recommendations set forth by the POLARIS, and whether its established rules prove effective in practice, remains insufficiently verified. As the number of Arctic ship operations increases and the accumulation of multi-year AIS data, the database for assessing the effectiveness of the POLARIS has been enhanced. In this study, the relationship between ship navigation speed and sea ice RIO was analyzed, and the compliance of ice-class ships with the POLARIS was quantified based on sea ice and AIS data.

5.1 Influencing factors on RIO

In quantifying sea ice risks, the quantitative framework of the AIRSS was adopted by the POLARIS, which implies that its current formulations for the RIO and IN overlook the critical risk factor of ship type. When a ship accident occurs, even if the ship is of the same ice-class, the Tanker will cause more serious consequences, but the POLARIS ignores the type differences between ships (Heikkilä et al., 2024; Xu et al., 2021; Gan et al., 2023). Shu et al. (2024) demonstrated that variations in ship type lead to substantial differences in navigation speed under sea ice conditions. Due to differences in ship scale and structural strength, Cargo and Tanker ships exhibit markedly higher navigation speeds in ice-covered waters compared to Fishing ships and Other ships. In this study, ice-class ships complying with the POLARIS guidelines

were categorized by ship type, and the resultant speed distributions are consistent with the findings of Shu et al. (2024). This result indicates that the overall speed of ships of the same ice-class but different types tend to decrease with the increase of sea ice risk. This result provides full verification of the significant impact exerted by differences in ship ice-class and type on navigation speed. In addition, from the speed statistics of PC7 ice-class Tankers in different SIC and SIT ranges (see Fig. 10), the speed is more sensitive to the fluctuation of SIT than SIC. Ship speed shows a marked decline only when SIC exceeds 80%, whereas a significant reduction is observed when ships encounter ice with a SIT greater than 0.7 m. Consequently, the exclusive consideration of ship ice-class and sea ice conditions in the RIO calculation is incomplete. Differentiating between ship types and providing navigation guidance suggestions are important directions for enhancing the POLARIS and its management mechanism. Moreover, improving the RIO calculation model to make it more sensitive to SIC is another key area for improvement.

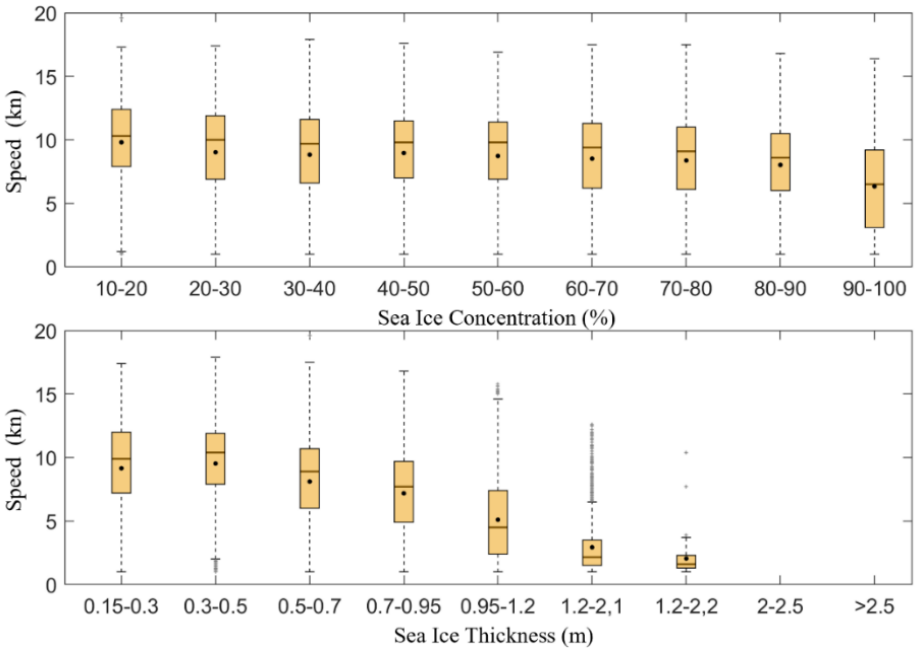

Fig. 10. Relationship between the speed of PC7 ice-class Tanker ships and sea ice conditions.

5.2 Spatio-temporal characteristics of the non-compliance events

The safe control zones and navigable windows criteria previously utilized in the 2020 Rules and AIRSS assessment frameworks were not adopted by the POLARIS. Statistical analyses of non-compliance rates indicate that the division of risk intervals indeed exerts a constraining effect on ship navigational behavior. Furthermore, the study into the spatio-temporal distribution of non-compliance events reveals clear regularities, from which several high-incidence areas and periods have been identified. Taking IA Super ice-class ships as an example, the main non-compliance hotspots are identified as the Kara Strait and the Kara Sea, located between the northern part of Novaya Zemlya and the Yamal Peninsula. These regions are classified as the second and sixth control zones under the 2020 Rules (RFGD, 2020). Since IA Super ice-class ships fall between ice-classes Arc4 and Arc5 and are subject to these regulations, they are prohibited from navigating under heavy ice conditions. Therefore, this study

759 suggests that the delineation and management of safe control zones hold considerable
760 referential value. It also provides useful insights on the future development of
761 emergency and rescue stations (ERS) along the coasts of the Arctic navigational routes.

762 From a temporal perspective, with the accelerated melting of sea ice, a noticeable
763 reduction in non-compliance events has been observed beginning in July. By the Rules
764 in NSR, navigable time windows have been established for certain ships (Zhang et al.,
765 2016), the navigable windows are shown in Fig. 11. The results presented in Fig. 11.
766 indicate that the navigable period for most ice-class ships spans from July to November,
767 during which sea ice conditions are at annual minimum. However, some ice-class ships
768 non-compliance the rules during the navigation period, such as IA Super and IA ice-
769 class ships. The non-compliance events occurred in areas with latitudes exceeding 80°,
770 the sea ice did not pose a threat to ships sailing along the main shipping channel. Lin et
771 al. (2024) summarized historical literature and concluded that the navigation windows
772 for most ships in the Northeast Passage (NEP) are from July to October, which is quite
773 different from the actual results. Therefore, further improvements to the POLARIS
774 could draw on the regional management approach from the NSR Rules. By integrating
775 regional sea ice conditions, navigational windows for each zone can be delineated,
776 thereby enabling effective spatio-temporal management of Arctic ship operations.
777 Development of ERS is essential for sustained and sustainable Arctic shipping
778 operations. The spatio-temporal analysis result in this section will aid significant
779 policy-making decision not only on the ESR location selection but also the resource

optimization across different ESRs at different seasons/months, contributing to cross-regions/countries collaborations.

Ice class of the ship	Ice navigation method	Water area of the Northern Sea Route[2]						
		1, 2, 3, 4, 5, 6, 7	8, 9, 10, 11	12, 13, 14	15, 16, 17	18, 19, 20, 21	22, 23, 24, 27	25, 26, 28
		HMLC	HMLC	HMLC	HMLC	HMLC	HMLC	HMLC
Arc4	IN	-*++	--++	--++	--++	--++	--++	-*++
	NI	++++	++++	-+++	-+++	-+++	-+++	-+++
Arc5	IN	-*++	--++	--++	--++	--++	--++	-*++
	NI	++++	++++	-+++	-+++	-+++	-+++	-+++
Arc6	IN	*+++	-*++	-*++	-*++	-*++	-*++	-*++
	NI	++++	++++	-+++	-+++	-+++	-+++	-+++
Arc7	IN	++++	*+++	*+++	*+++	*+++	*+++	*+++
	NI	++++	++++	++++	++++	++++	++++	++++
Arc8	IN	++++	++++	*+++	*+++	*+++	*+++	++++
	NI	++++	++++	++++	++++	++++	++++	++++
Arc9	IN	++++	++++	++++	++++	++++	++++	++++
	NI	++++	++++	++++	++++	++++	++++	++++

Fig. 11. Criteria for admission of ships in the area of the NSR for ships with ice-classes Arc4-Arc9 (RFGD, 2020). IN: independent navigation; NI: navigation under icebreaker assistance; H: heavy type of ice conditions; M: medium type of ice conditions; L: light type of ice conditions; C: clean water; +: navigation of the ship is permitted; -: navigation of the ship is prohibited; *: independent navigation is allowed from July the 1st to November the 30th.

5.3 Policy implications

Due to the special geographical location of the Arctic, cross-border shipping management coordination is particularly important. A unified standard framework for international shipping safety management was provided by the POLARIS. In order to further refine the application of the POLARIS in assessing sea ice risks, this study outlines several avenues for enhancing future Arctic ship management policies, addressing multiple dimensions including ice condition classification, ship categorization, and navigational area management. Another important policy response is to assess the effectiveness of models and rules in a data-driven manner by correlating and fusing large-scale multi-source data. The validation process is made more

798 comprehensive and accurate by this data fusion, and the POLARIS is provided with a
799 dynamic feedback mechanism to ensure its long-term effectiveness and adaptability in
800 the changing Arctic waters. Research findings indicate that many ships engage in non-
801 compliant behavior in high-risk areas, particularly in regions characterized by dense
802 sea ice and complex navigation conditions. High-incidence regions of non-compliance
803 were identified through the analysis of AIS and sea ice data. Based on these
804 observations, supervision of these high-risk areas was recommended to be strengthened.
805 The dynamic risk assessment provided by the POLARIS is employed to conduct real-
806 time monitoring and to promptly stop non-compliant operations, thereby ensuring that
807 ships are always operated within a safe range. A basis for formulating navigation
808 standards in different ice areas is provided through the analysis of AIS, sea ice, and
809 navigation behavior data of Arctic ships accumulated over the years. In addition,
810 continuous data support for the dynamic updating of navigation manuals is offered by
811 this analysis.

812 The effectiveness of POLARIS in guiding ship navigation in actual ice-covered
813 regions was assessed in this study. Although the POLARIS plays a crucial role in
814 assessing sea ice risks, it cannot be solely relied upon to determine whether navigational
815 conditions are safe (Fedi et al., 2018a; Müller et al., 2023; Gan et al., 2025). In addition,
816 due to the limitations of the spatio-temporal resolution of sea ice data and the failure to
817 distinguish between icebreaker pilotage and ship formation, these factors will affect the
818 results of the ice speed distribution.

6. Conclusion

The effectiveness of the POLARIS was assessed based on the characteristics of Arctic shipping traffic. The sea ice data and AIS data from the Arctic areas during the 2018 to 2022 were collected in this study. Spatio-temporal correlation was then employed to investigate the behavioral characteristics of Arctic ships, their compliance with the POLARIS, and the spatio-temporal distribution of non-compliance events. The results show that the sea ice extent affects the distribution of ship navigation trajectories, while the speed is greatly restricted by the sea ice conditions. In addition, high ice-classes ships (PC2, PC3, and PC5) all complied with the speed recommended by the POLARIS during actual navigation, and verified that ship type is an important factor in assessing sea ice risk. Moreover, speed non-compliance rates for ice-class ships PC4, PC6, and PC7 were found to be 68.21%, 67.00%, and 66.18%, respectively. This study further analyzed the spatio-temporal distribution of non-compliant ships The results revealed the high-incidence areas of ice-class ship non-compliance, among which the most non-compliance events occurred in the waters of the Kara Strait. Moreover, a time series analysis of these non-compliance events confirmed that the navigational windows for most ice-classes ships are concentrated between July and November, while some non-compliance events during these periods are clustered in areas north of 80°N. Therefore, the navigation rules of ice-class ships in the Arctic are revealed, and the effectiveness of the POLARIS in guiding actual ship navigation is assessed in this study. A theoretical basis for developing a more comprehensive ice navigation guidance

manual is also developed and provided.

The impact of sea ice on ship navigation behavior is the main focus of the research, and only a quantitative model of sea ice risk is given in the POLARIS. However, it was observed that some ship behavior records are associated with multiple factors beyond sea ice conditions alone, including but not limited to ambient low temperatures, sea fog, communication capabilities, and the pivotal role of icebreaker escorting. Future research will incorporate these factors to further investigate the navigational behavior characteristics of ships in ice-covered regions.

Acknowledgements

This work was supported by the National Natural Science Foundation of China (NSFC) under Grant No.52271369, No.42407114, and a European Research Council project under the European Union's Horizon 2020 research and innovation program (TRUST CoG 2019 864724).

References

Aksenov, Y., Popova, E. E., Yool, A., Nurser, A. G., Williams, T. D., Bertino, L., Bergh, J., 2017. On the future navigability of Arctic sea routes: High-resolution projections of the Arctic Ocean and sea ice. Marine Policy 75, 300-317.

Akbayirli, K., Okan, T., 2022. How do practitioners view Arctic shipping Routes? a cognitive appraisal approach. Transportation Research Part D: Transport and Environment 110, 103432.

Bartenstein, K., Dremliuga, R., Prisekina, N., 2022. Regulation of Arctic shipping in Canada and Russia. Arctic Review on Law and Politics 13, 338-360.

Bhagwat, J. V., Khalturinskaya, V. A., 2023. Evolution of Russian State Policy for Development of the NSR (2018–2022): Influence of Geopolitical and Geoeconomic Factors. Social and Economic Development (51), 98-132.

Bond, J., Hindley, R., Kendrick, A., Kämäräinen, J., Kuulila, L. 2018. Evaluating risk and determining operational limitations for ships in ice. Offshore Technology Conference, OTC-29143-MS, Houston, Texas, USA.

Bond J, Oldford D, Kelly L., 2022. Postulating an Update to Canada's Zone/Date System. SNAME Maritime Convention, Houston, Texas, USA.

Boylan, B. M., 2021. Increased maritime traffic in the Arctic: Implications for governance of Arctic sea routes. Marine Policy 131, 104566.

Browne, T., Tran, T. T., Veitch, B., Smith, D., Khan, F., Taylor, R., 2022. A method for evaluating operational implications of regulatory constraints on Arctic shipping.

874 Marine Policy 135, 104839.
875 Canada, 2010. Consolidated federal laws of Canada, Shipping Safety Control Zones
876 Order (C.R.C., c. 356).
877 Transport Canada, 2018. Arctic Ice Regime Shipping System (AIRSS) standard. TP
878 14044.
879 Cao, Y., Liang, S., Sun, L., Liu, J., Cheng, X., Wang, D., Chen, Y., Yu, M., Feng, K.,
880 2022. Trans-Arctic shipping routes expanding faster than the model projections.
881 Global Environmental Change 73, 102488.
882 CHNL, 2024. Main Results of NSR Transit Navigation in 2024. Centre for High North
883 Logistics.
884 CMEMS, 2024. Global Ocean Ensemble Physics Reanalysis. E.U. Copernicus Marine
885 Service Information. DOI: 10.48670/moi-00024.
886 Chen, J. L., Kang, S. C., Wu, A. D., & Hu, D. D., 2023. Impacts of 1.5° C global
887 warming on hydrological conditions of navigation along the Northern Sea Route
888 and Northwest Passage. Advances in Climate Change Research, 14(6), 904-912.
889 Chen, S., Meng, B., Qiu, B., Kuang, H., 2025. Dynamic effects of maritime risk on
890 macroeconomic and global maritime economic activity. Transport Policy 167, 246–
891 263.
892 Chen, X., Patel, M., Xu, L., Chen, Y., Scott, K. A., Clausi, D. A., 2025. A Weakly
893 Supervised Learning Approach for Sea Ice Stage of Development Classification
894 from AI4Arctic Sea Ice Challenge Dataset. IEEE Transactions on Geoscience and

Remote Sensing.

Copland, L., Dawson, J., Tivy, A., Delaney, F., Cook, A., 2021. Changes in shipping navigability in the Canadian Arctic between 1972 and 2016. Facets 6(1), 1069-1087.

Diebold, F. X., Rudebusch, G. D., Göbel, M., Coulombe, P. G., Zhang, B., 2023. When will Arctic sea ice disappear? Projections of area, extent, thickness, and volume. Journal of Econometrics 236(2), 105479.

Fedi, L., Etienne, L., Faury, O., Rigot Muller, P., Stephenson, S., Cheaitou, A., 2018a. Arctic navigation: stakes, benefits and limits of the POLARIS system. The Journal of Ocean Technology 13(4), 54-67.

Fedi, L., Faury, O., Gritsenko, D., 2018b. The impact of the Polar Code on risk mitigation in Arctic waters: a “toolbox” for underwriters?. Maritime Policy & Management 45(4), 478-494.

Gan, L., Ye, B., Huang, Z., Xu, Y., Chen, Q., & Shu, Y., 2023. Knowledge graph construction based on ship collision accident reports to improve maritime traffic safety. Ocean & Coastal Management, 240, 106660.

Gan, L., Gao, Z., Zhang, X., Xu, Y., Liu, R. W., Xie, C., & Shu, Y., 2025. Graph neural networks enabled accident causation prediction for maritime vessel traffic. Reliability Engineering & System Safety, 257, 110804.

He, Y., Shu, Q., Wang, Q., Song, Z., Zhang, M., Wang, S., Zhang, L., Bi, H., Pan, R., Qiao, F., 2024. Arctic Amplification of marine heatwaves under global warming. Nature Communications 15(1), 8265.

916 Heikkilä, M., Grönholm, T., Majamäki, E., Jalkanen, J.-P., 2024. Effect of ice class to
917 vessel fuel consumption based on real-life MRV data. Transport Policy 148, 168–
918 180.
919 Howell, S. E., Yackel, J. J., 2004. A vessel transit assessment of sea ice variability in
920 the Western Arctic, 1969–2002: implications for ship navigation. Canadian Journal
921 of Remote Sensing 30(2), 205-215.
922 IMO, 2016. Guidance on methodologies for assessing operational capabilities and
923 limitations in ice. International Maritime Organization, London, UK,
924 MSC.1/Circ.1519.
925 IMO, 1974. International Convention for the Safety of Life at Sea. International
926 Maritime Organization, London, UK.
927 Jiacai, P. A. N., Mengjie, L. U., & Feng, M. A., 2025. Review of ship navigational safety
928 in the Arctic Northwest passage. Regional Studies in Marine Science, 87, 104229.
929 Koçak, S.T., Yercan, F., 2021. Comparative cost-effectiveness analysis of Arctic and
930 international shipping routes: A Fuzzy Analytic Hierarchy Process. Transport
931 policy 114, 147–164.
932 Kubat, I., Collins, A., Gorman, B., Timco, G., 2005. A methodology to evaluate
933 Canada's Arctic shipping regulations. In International Conference on Port and
934 Ocean Engineering under Arctic Conditions (POAC).
935 Kujala, P., Kämäräinen, J., Suominen, M., 2019. Validation of the new risk based design
936 approaches (POLARIS) for Arctic and Antarctic operations. International

Conference on Port and Ocean Engineering under Arctic Condition.

Kulesh, V.A., Ogay, S.A., Voyloshnikov, M.V., 2013. Safety of Ships Navigation in Ice and Operational Effectiveness. ISOPE International Ocean and Polar Engineering Conference. ISOPE-I-13-092.

Lee, H.-W., Roh, M.-I., Kim, K.-S., 2021. Ship route planning in Arctic Ocean based on POLARIS. Ocean Engineering 234, 109297.

Li, Z., Yao, C., Zhu, X., Gao, G., Hu, S., 2022. A decision support model for ship navigation in Arctic waters based on dynamic risk assessment. Ocean Engineering 244, 110427.

Lin, B., Zheng, M., Chu, X., Mao, W., Zhang, D., Zhang, M., 2024. An overview of scholarly literature on navigation hazards in Arctic shipping routes. Environmental Science and Pollution Research 31(28), 40419-40435.

Lindstad, H., Bright, R.M., Strømman, A.H., 2016. Economic savings linked to future Arctic shipping trade are at odds with climate change mitigation. Transport Policy 45, 24–30.

Liu, C., Kulkarni, K., Suominen, M., Kujala, P., Musharraf, M., 2024. On the data-driven investigation of factors affecting the need for icebreaker assistance in ice-covered waters. Cold Regions Science and Technology 221, 104173.

Liu, C., Liu, J., Zhou, X., Zhao, Z., Wan, C., Liu, Z., 2020. AIS data-driven approach to estimate navigable capacity of busy waterways focusing on ships entering and leaving port. Ocean Engineering 218, 108215.

Liu, H., Wu, C., Li, B., Zong, Z., Shu, Y., 2025. Research on Ship Anomaly Detection Algorithm Based on Transformer-GSA Encoder. IEEE Transactions on Intelligent Transportation Systems 1–12.

Marchenko, N., 2014. Northern sea route: Modern state and challenges. International conference on offshore mechanics and Arctic engineering. American Society of Mechanical Engineers 45561: V010T07A022.

Mudryk, L.R., Dawson, J., Howell, S.E., Derksen, C., Zagon, T.A., Brady, M., 2021. Impact of 1, 2 and 4 C of global warming on ship navigation in the Canadian Arctic. Nature Climate Change 11, 673–679.

Müller, M., Knol-Kauffman, M., Jeuring, J., Palerme, C., 2023. Arctic shipping trends during hazardous weather and sea-ice conditions and the Polar Code's effectiveness. npj Ocean Sustainability 2(1), 12.

RFGD. 2020, Rules of navigation in the water area of the Northern Sea Route, Russian Federation Government, No. 1487.

Shu, Y., Cui, H., Song, L., Gan, L., Xu, S., Wu, J., Zheng, C., 2024. Influence of sea ice on ship routes and speed along the Arctic Northeast Passage. Ocean & Coastal Management 256, 107320.

Shu, Y., Huang, F., Wu, J., Chen, J., Song, L., Gan, L., Yang, Z., 2025. Research on Ship Following Behavior Based on Data Mining in Arctic Waters. IEEE Transactions on Intelligent Transportation Systems 1–11.

Shu, Y., Zhu, Y., Xu, F., Gan, L., Lee, P.T.-W., Yin, J., Chen, J., 2023. Path planning for

ships assisted by the icebreaker in ice-covered waters in the Northern Sea Route based on optimal control. Ocean Engineering 267, 113182.

Sibul, G., Schütz, P., & Fagerholt, K., 2026. Arctic route planning under ice uncertainty: A risk-averse stochastic shortest path problem. Transportation Research Part E: Logistics and Transportation Review, 205, 104507.

Similä, M., Lensu, M., 2018. Estimating the Speed of Ice-Going Ships by Integrating SAR Imagery and Ship Data from an Automatic Identification System. Remote Sensing 10, 1132.

Solski, J.J., 2023. The Polar Code Process and Sovereignty Bargains: Comparing the Approaches of Canada and Russia to POLARIS. Ocean Development & International Law 54, 111–134.

Stoddard, M. A., Etienne, L., Fournier, M., Pelot, R., Beveridge, L., 2016. Making sense of Arctic maritime traffic using the polar operational limits assessment risk indexing system (POLARIS). IOP Conference series: Earth and environmental science 34(1): 012034.

Tarovik, O., Yakimov, V., Dobrodeev, A., Li, F., 2022. Influence of seasonal and regional variation of ice properties on ship performance in the Arctic. Ocean Engineering 257, 111563.

Timco, G.W., Kubat, I., 2001. Canadian ice regime system: improvements using an interaction approach. Proceedings of the International Conference on Port and Ocean Engineering Under Arctic Conditions.

1000 Todorov, A., 2022. Dire straits of the Russian Arctic: Options and challenges for a
1001 potential US FONOP in the Northern Sea Route. Marine Policy 139, 105020.
1002 Vylegzhanin, A. N., Nazarov, V. P., Bunik, I. V., 2020. The Northern Sea route: Solving
1003 political and legal problems. Herald of the Russian Academy of Sciences, 90, 718-
1004 729.
1005 Wang, B., Liu, Y., Dai, W., Li, J., 2025. Incremental route planning based on daily risk
1006 assessment for Arctic navigation. Ocean Engineering 320, 120294.
1007 Wang, L., Li, Y., Wan, Z., Yang, Z., Wang, T., Guan, K., Fu, L., 2020. Use of AIS data
1008 for performance evaluation of ship traffic with speed control. Ocean Engineering
1009 204, 107259.
1010 Wang, Y., Liu, K., Zhang, R., Qian, L., Shan, Y., 2021. Feasibility of the Northeast
1011 Passage: The role of vessel speed, route planning, and icebreaking assistance
1012 determined by sea-ice conditions for the container shipping market during 2020–
1013 2030. Transportation Research Part E: Logistics and Transportation Review 149,
1014 102235.
1015 Wang, Y., You, J., Cui, M., Qiu, Y., Liao, H., Luo, Y., & Zhang, F., 2026. A multi-
1016 objective route planning method for polar sea based on the NSGA-III algorithm.
1017 Ocean Engineering, 343, 123199.
1018 Xu, S., Kim, E., Haugen, S., 2021. Review and comparison of existing risk analysis
1019 models applied within shipping in ice-covered waters. Safety science 141, 105335.
1020 Yakimov, V.V., 2023. A concept for onboard risk-based information system to ensure

the safety of ship operation in ice conditions. AIP Conference Proceedings. AIP Publishing, 2700(1).

Yang, X., Lin, Z.Y., Zhang, W.J., Xu, S., Zhang, M.Y., Wu, Z.D., Han, B., 2024. Review of risk assessment for navigational safety and supported decisions in arctic waters. Ocean & Coastal Management 247, 106931.

Ye, L., Chen, X., Liu, H., Zhang, R., Li, J., Lu, C., Zhao, Y., 2024. A Study of Multi-Step Sparse Vessel Trajectory Restoration Based on Feature Correlation. Applied Sciences 14, 4057.

Zhang, X., Zhao, N., Dai, Z., Han, Z., 2025. Satellites reveal different stories of marine heatwaves in the sea-ice-covered pan-Arctic. Communications Earth & Environment 6(1), 17.

Zhou, L., Sun, Q., Ding, S., Han, S., Wang, A., 2023. A Machine-Learning-Based Method for Ship Propulsion Power Prediction in Ice. Journal of Marine Science and Engineering 11, 1381.

Zhou, L., Gao, J., Xu, S., Bai, X., 2018. A numerical method to simulate ice drift reversal for moored ships in level ice. Cold Regions Science and Technology 152, 35–47.

Zhang, Y., Meng, Q., Zhang, L., 2016. Is the Northern Sea Route attractive to shipping companies? Some insights from recent ship traffic data. Marine Policy 73, 53–60.